MOLECULAR AND CELLULAR BIOLOGY, June 2010, p. 2636–2650 Vol. 30, No. 11
0270-7306/10/$12.00 doi:10.1128/MCB.01194-09


# NADPH Oxidase 1 Modulates WNT and NOTCH1 Signaling To Control the Fate of Proliferative Progenitor Cells in the Colon[▽]

Nicolas Coant,[1,2]† Sanae Ben Mkaddem,[1,2]† Eric Pedruzzi,[1,2] Cécile Guichard,[1,2] Xavier Tréton,[1,2] Robert Ducroc,[1,2] Jean-Noel Freund,[3] Dominique Cazals-Hatem,[4] Yoram Bouhnik,[1,2,5] Paul-Louis Woerther,[6] David Skurnik,[6] Alain Grodet,[1,2] Michèle Fay,[1,2] Denis Biard,[7] Thécla Lesuffleur,[8] Christine Deffert,[9] Richard Moreau,[1,2] André Groyer,[1,2] Karl-Heinz Krause,[9] Fanny Daniel,[1,2]† and Eric Ogier-Denis[1,2]*†

*INSERM, U773, Centre de Recherche Bichat Beaujon CRB3, BP 416, F-75018 Paris, France[1]; Université Denis Diderot Paris 7, site Bichat, BP 416, F-75018 Paris, France[2]; INSERM, U682, Université Louis Pasteur, UMR S682, 3 avenue Molière, 67000 Strasbourg, France[3]; Service d'Anatomo-Pathologie, Hôpital Beaujon, 100 Blvd. du Général Leclerc, Clichy, 92110 Clichy Cedex, France[4]; Service de Gastroentérologie et d'Assistance Nutritive, PMAD Hôpital Beaujon, 100 Blvd. du Général Leclerc, Clichy la Garenne, 92110 Clichy Cedex, France[5]; Laboratoire de Bactériologie, Hôpital Bichat-Claude Bernard, AP-HP, Université Paris 7 Denis Diderot, 46 rue Henri Huchard, 75018 Paris, France[6]; CEA-DSV-iRCM/INSERM U935, Institut A. Lwoff-CNRS, BP 8, 94801 Villejuif Cedex, France[7]; UMR S938, Centre de Recherche de Saint-Antoine, Paris F-75012, France, and UPMC Université Paris 06, Paris F-75005, France[8]; and Department of Pathology and Immunology, Geneva Medical Faculty and University Hospitals, 1211 Geneva 4, Switzerland[9]*

Received 3 September 2009/Returned for modification 14 December 2010/Accepted 21 March 2010

**The homeostatic self-renewal of the colonic epithelium requires coordinated regulation of the canonical Wnt/β-catenin and Notch signaling pathways to control proliferation and lineage commitment of multipotent stem cells. However, the molecular mechanisms by which the Wnt/β-catenin and Notch1 pathways interplay in controlling cell proliferation and fate in the colon are poorly understood. Here we show that NADPH oxidase 1 (NOX1), a reactive oxygen species (ROS)-producing oxidase that is highly expressed in colonic epithelial cells, is a pivotal determinant of cell proliferation and fate that integrates Wnt/β-catenin and Notch1 signals. NOX1-deficient mice reveal a massive conversion of progenitor cells into postmitotic goblet cells at the cost of colonocytes due to the concerted repression of phosphatidylinositol 3-kinase (PI3K)/AKT/Wnt/β-catenin and Notch1 signaling. This conversion correlates with the following: (i) the redox-dependent activation of the dual phosphatase PTEN, causing the inactivation of the Wnt pathway effector β-catenin, and (ii) the downregulation of Notch1 signaling that provokes derepression of mouse atonal homolog 1 (Math1) expression. We conclude that NOX1 controls the balance between goblet and absorptive cell types in the colon by coordinately modulating PI3K/AKT/Wnt/β-catenin and Notch1 signaling. This finding provides the molecular basis for the role of NOX1 in cell proliferation and postmitotic differentiation.**

Self-renewal of the colonic epithelium involves coordinated cellular processes, such as proliferation, differentiation, migration, and cell death, to ensure homeostasis. Colonic epithelial stem cells self-renew throughout life, cycling infrequently to produce more committed proliferating precursors that actively divide in the lower part of the crypts. After upward migration and cell cycle arrest, these transit-amplifying precursor cells differentiate into two cell lineages (i.e., the absorptive colonocytes and secretory cells). The secretory lineage can be further subdivided into mucus-secreting goblet cells and hormone-secreting enteroendocrine cells. Correlative studies suggest that highly evolutionarily conserved signaling pathways, such as the Wnt/β-catenin and Notch cascades, function together to control continuous proliferation of the crypt cell population and differentiation of individual cells (8, 11, 40, 51, 59, 61). The specification of precursor cells into colonocytes is determined in part by the transcription factor Hes1, while the differentiation of secretory precursors into goblet or enteroendocrine cells is regulated by Math1 or neurogenin 3, respectively, all of which are transcriptional targets of Notch signaling (19, 20, 50, 65). The canonical Wnt/β-catenin signaling pathway is believed to be the major signaling cascade controlling different processes: maintaining stem/progenitor cells via cell cycle control and inhibition of differentiation, controlling migration and localization of epithelial cells along the crypt-villus axis, and directing secretory lineage development as well as terminal differentiation of Paneth cells in the small intestine (reviewed in references 9, 44, and 51). Although the Wnt/β-catenin and Notch signaling pathways seem to be essential for stem cell function and maintenance, the mechanisms by which Wnt/β-catenin and Notch signaling synergize to regulate self-renewal and homeostasis in the colon remain elusive.

NOX1, a member of the reactive oxygen species (ROS)-generating NADPH oxidase family, is expressed at high levels in colonic epithelial cells (16, 23, 57) and is absent (22) or barely detectable (28) in normal small intestinal mucosa. *NOX1* mRNA expression is detected either along the crypt-to-

* Corresponding author. Mailing address: INSERM, U773, Centre de Recherche Bichat Beaujon, CRB3, BP 416, 16 rue Henri Huchard, Paris 75018, France. Phone: (331) 5727-7307. Fax: (331) 5727-7461. E-mail: eric.ogier-denis@inserm.fr.
† These authors contributed equally to this work.
▽ Published ahead of print on 29 March 2010.

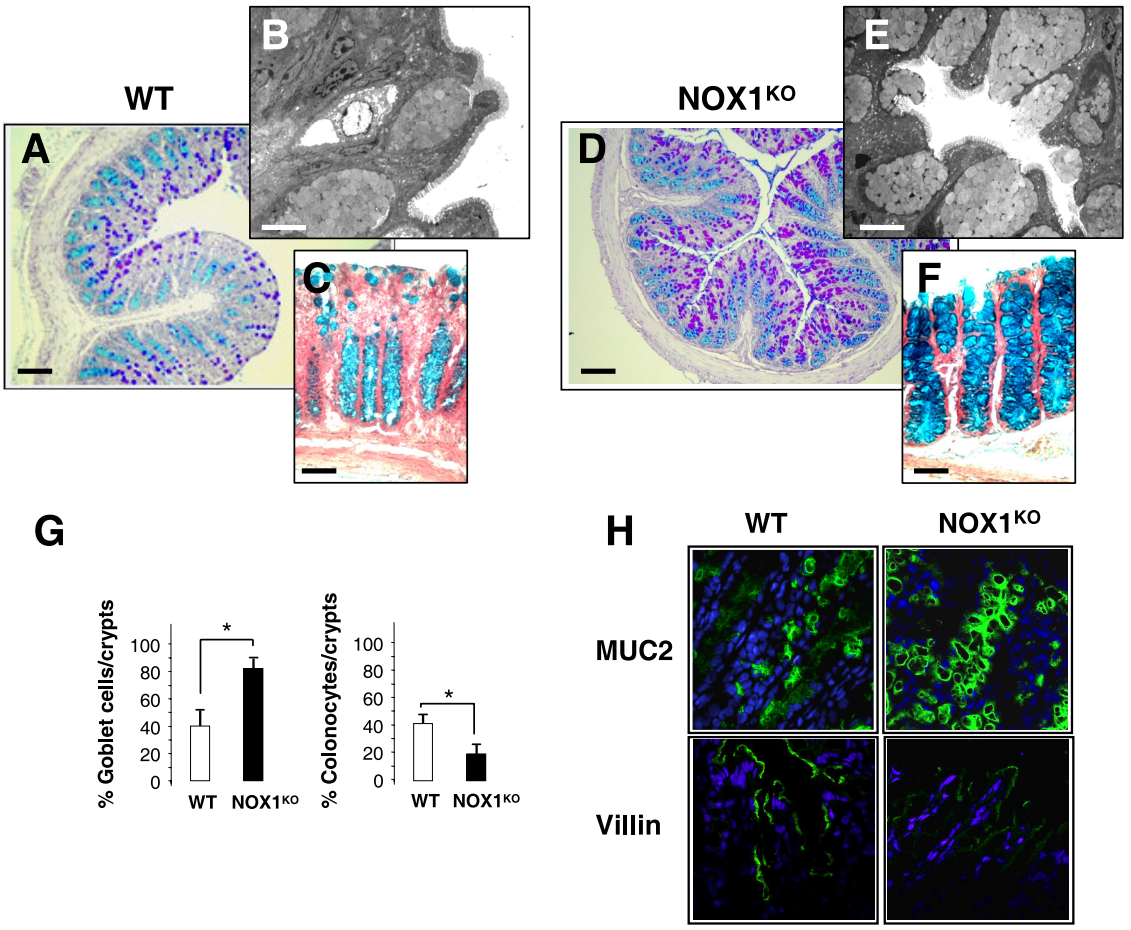


FIG. 1. NOX1$^{KO}$ mice exhibit upregulation of goblet cells. Representative sections of distal colon from wild-type (WT) (A and C) or NOX1$^{KO}$ (D and F) mice stained with periodic acid-Schiff and Alcian blue (A and D) or Alcian blue alone (C and F) show marked accumulation of goblet cells in NOX1$^{KO}$ mice. Ultrastructural examination of colonic sections processed for transmission electron microscopy reveals a higher density of goblet cells in NOX1$^{KO}$ mice (E) than in WT mice (B). (G) Eight crypts per section with 2 individual sections from each animal were counted. The percentage of goblet cells and colonocytes per crypt is represented as mean ± SEM ($n$ = 15 for WT and $n$ = 13 for NOX1$^{KO}$ mice); *, significantly different from the WT ($P < 0.001$), Student's $t$ test. (H) Confocal microscopy with anti-MUC2 (green) and antivillin (green) in sections from the distal colon shows accumulation of goblet cells at the expense of colonocytes in NOX1$^{KO}$ mice and is consistent with the data presented in panel G. Nuclei (blue) were stained with DAPI. Photomicrographs shown here are representative sections from 10 animals per group. Scale bar, 100 μm (A and D), 50 μm (C and F) or 5 μm (B and E). Original magnification, ×60 (H).

cuff axis in human colon epithelial cells (57, 60) or within the lower two-thirds of mouse colon crypts (16) and follows an anterior-posterior gradient with the highest levels in the distal colon (4, 57, 60). In a variety of cell types, NOX1 plays a role in host defense, cell growth and differentiation, cell migration, and malignant transformation (5, 32, 45, 48). However, its function in the distal gastrointestinal tract is not understood and remains a matter of debate (5). Basically, there are three major working hypotheses: a role in host defense based on the observation that NOX1 expression is enhanced by gamma interferon (INF-γ) (16), lipopolysaccharide (LPS) (22), or flagellin (46) and a role in the regulation of cell proliferation. A role of NOX1 as a mitogenic oxidase in nonintestinal cell types has been suggested (1, 56). However, NOX1 expression is increased upon differentiation in cultured colon cancer cell lines (16) and shows a differentiation-dependent expression pattern in well-differentiated adenocarcinomas (13). Moreover, NOX1 is overexpressed in human colon cancers (especially at the early adenoma stages [21]) and correlates with activating mutations in K-Ras (28). Thus, by a variety of unidentified mechanisms, NOX1 might modulate transduction signals that may be instrumental in the balance between colonic cell proliferation and differentiation. Accordingly, using NOX1-deficient (NOX1$^{KO}$) mice (15) as an experimental model, our objective was to elucidate whether or not NOX1 is involved in the homeostasis of the colonic epithelium.

## MATERIALS AND METHODS

**Animals and treatments.** NOX1$^{KO}$ mice were backcrossed into the C57BL/6 genetic background for at least seven generations. Wild-type and NOX1$^{KO}$ mice were used between 8 and 10 weeks of age. BrdU (Sigma) was injected intraperitoneally (i.p.) at 100 μg/g animal body weight 1 h or 24 h prior to sacrifice. Insulin growth factor 1 (IGF1) administration was carried out using medium-grade human Long-Arg$^3$-IGF1 (LR$^3$IGF1) (GroPep), an IGF1 analogue with a decreased affinity for IGF binding proteins. The peptide was injected subcutaneously twice daily (2 μg/g every 12 h) for 4 days. The fourth day, the subcutaneous injection was followed 6 h later by an intraperitoneal injection to check for LR$^3$IGF1 efficiency. The mice were killed 30 min after the final injection.

TABLE 1. Electrical parameters and quantitative index of absorption and secretion in the NOX1$^{KO}$ mouse colon[a]

| Area analyzed and mouse group | Isc ($\mu$A/cm$^2$) | Conductance (mS/cm$^2$) | Response to challenge with: | |
|---|---|---|---|---|
| | | | Butyrate ($\Delta$Isc, $\mu$A/cm$^2$) | Carbachol ($\Delta$Isc, $\mu$A/cm$^2$) |
| Proximal colon | | | | |
| Wild-type mice | 41.7 ± 7.3 | 29.4 ± 3.6 | 4.2 ± 1.7 | 37.5 ± 9.5 |
| NOX1$^{KO}$ mice | 26.7 ± 5.9* | 29.5 ± 3.6 | 4.2 ± 1.1 | 9.2 ± 4.5* |
| Distal colon | | | | |
| Wild-type mice | 60.0 ± 14.3 | 33.4 ± 3.5 | 5.0 ± 1.8 | 95.0 ± 8.4 |
| NOX1$^{KO}$ mice | 36.0 ± 9.7* | 32.6 ± 4.2 | 5.3 ± 1.8 | 60.0 ± 14.0* |

[a] Note significant reductions of baseline short-circuit current (Isc) and carbachol-induced chloride secretion without change in conductance or absorption of butyrate in NOX1$^{KO}$ versus WT mice. Butyrate concentration, 10 mM; carbachol concentration, 100 mM. Data are means ± SEM of 3 separate experiments with sections of both proximal and distal colons from 6 animals per group. *, significantly different from the control value ($P < 0.05$) by one-way analysis of variance with the Turkey-Kramer multiple comparison post hoc test.

**Ethics statement.** Mice were bred and experimental procedures were carried out in accordance with the principles and guidelines established by the European Convention for the Protection of Laboratory Animals concerning the care and use of laboratory animals and with the authorization order no. B75-18-02 delivered by Ministry of Agriculture and Prefecture of Paris, France.

**RT-PCR analysis.** Total RNA was isolated from frozen distal colon using RNAble (Eurobio). Reverse transcription (RT) was carried out using Moloney murine leukemia virus (M-MLV) (Invitrogen). For PCR amplification, the thermocycler profile used consisted of an initial denaturation at 94°C for 2 min, followed by 25 to 35 cycles of 94°C (30 s), 55°C (30 s), and 72°C (60 s). Primer sequences are provided upon request.

**Cell culture.** HT-29Cl.16E and Caco-2 cells were grown for up to 25 days in Dulbecco's modified Eagle's medium (4.5 g/liter glucose) supplemented with 10 and 20% fetal calf serum, respectively, 100 $\mu$g/ml streptomycin, and 100 U/ml penicillin.

**Transfection.** HT-29Cl.16E cells were transfected by electroporation with pcDNA3-NOX1 or empty vector. Resistant clones were selected with 600 $\mu$g/ml G418 (Invitrogen) and then pooled after 3 weeks and maintained under G418 selection.

Caco-2 cells were transfected by electroporation with a pEBV-based small hairpin RNA (shRNA) *NOX1* vector. Sense and antisense oligodeoxynucleotides were as follows: shNOX1-Forward, 5′-GATCCCGACAGTGGAGTATGTGACATTCAAGAGAT-GTCACATACTCCACTGTCTTTTTTGGAAA-3′; shNOX1-Reverse, 5′-AGCTTTTCCAAAAAAGACAGTGGAGTATGTGACATCTCTTGAATGTCACATACTCCACTGTCGG. Cells were selected 48 h after transfection using hygromycin (300 $\mu$g/ml). The resistant clones were pooled after 3 weeks and maintained under hygromycin selection (sh-NOX1).

sh-NOX1 cells were transfected with PTEN or scrambled small interfering RNA (siRNA) (8 to 50 nM) (Qiagen) using Lipofectamine RNAimax (Invitrogen). SiRNA sequences were as follows: PTEN, 5′-CCAGUCAGAGGCGCUAUGU-3′; scrambled, 5′-UAGACCGGUAGUC-GGACCU-3′.

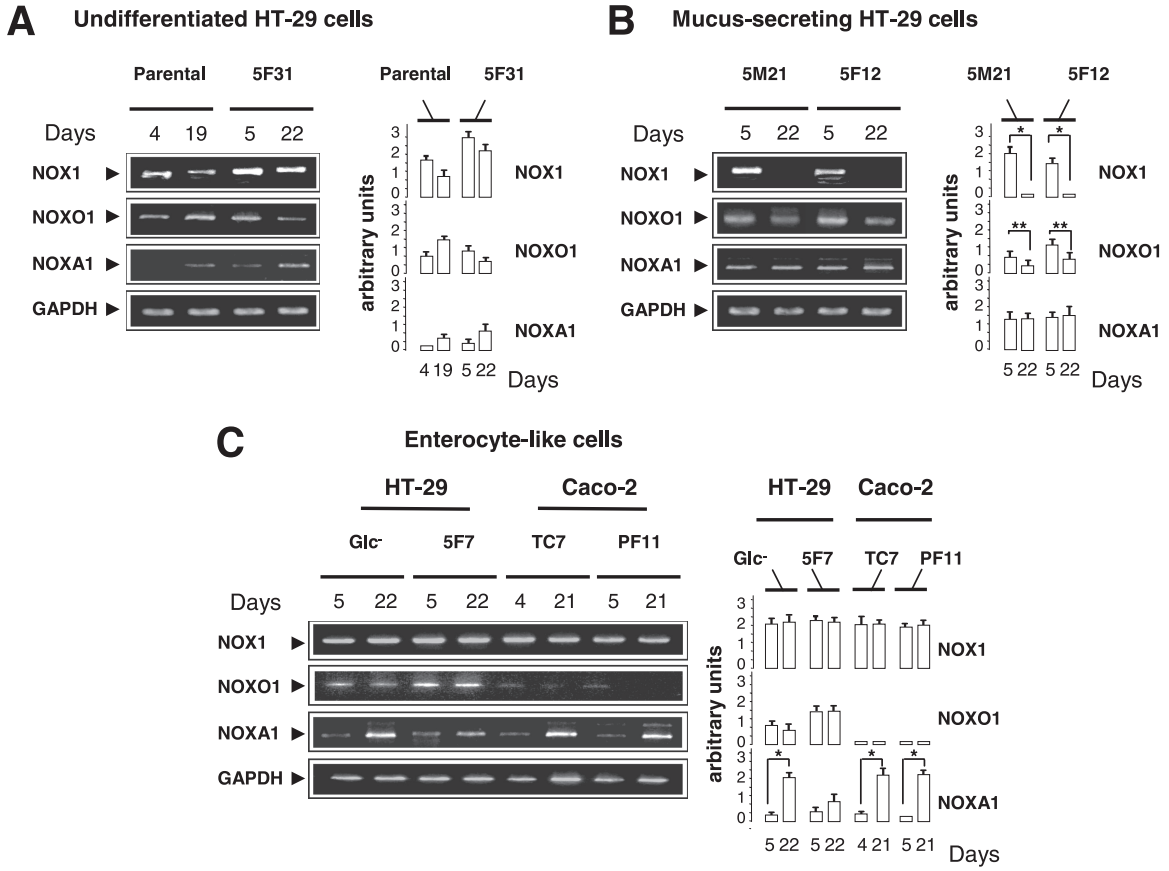


FIG. 2. Differentiation-dependent expression of NOX1 and regulatory partners in different mucus-secreting or enterocyte-like clones derived from parental HT-29 or Caco-2 cells. Semiquantitative RT-PCR shows the expression of *NOX1* and its regulatory partners: *NOXO1*, *NOXA1*, *p22$^{phox}$*, and *rac1* mRNA levels at days 4 and 5 (exponential phase of growth) and days 19 to 22 (confluence) in parental, 5-fluorouracil-resistant (5F31, 5F12, and 5F7) (31, 62), methotrexate-resistant (5M21) (31, 62), or nutrient deprivation (Glc$^-$) HT-29 cells and in Caco-2 cells (TC7 and PF11) (31, 62). These clones display an undifferentiated (A), mucus-secreting (B), or enterocyte-like phenotype (C). The *GAPDH* mRNA level was used as a loading control. The ratio of each mRNA level to that of *GAPDH* was quantified by scanning densitometry. Values are representative of 3 individual experiments performed in triplicate; means ± SEM are given. *, $P < 0.001$; **, $P < 0.01$ (Student's $t$ test).

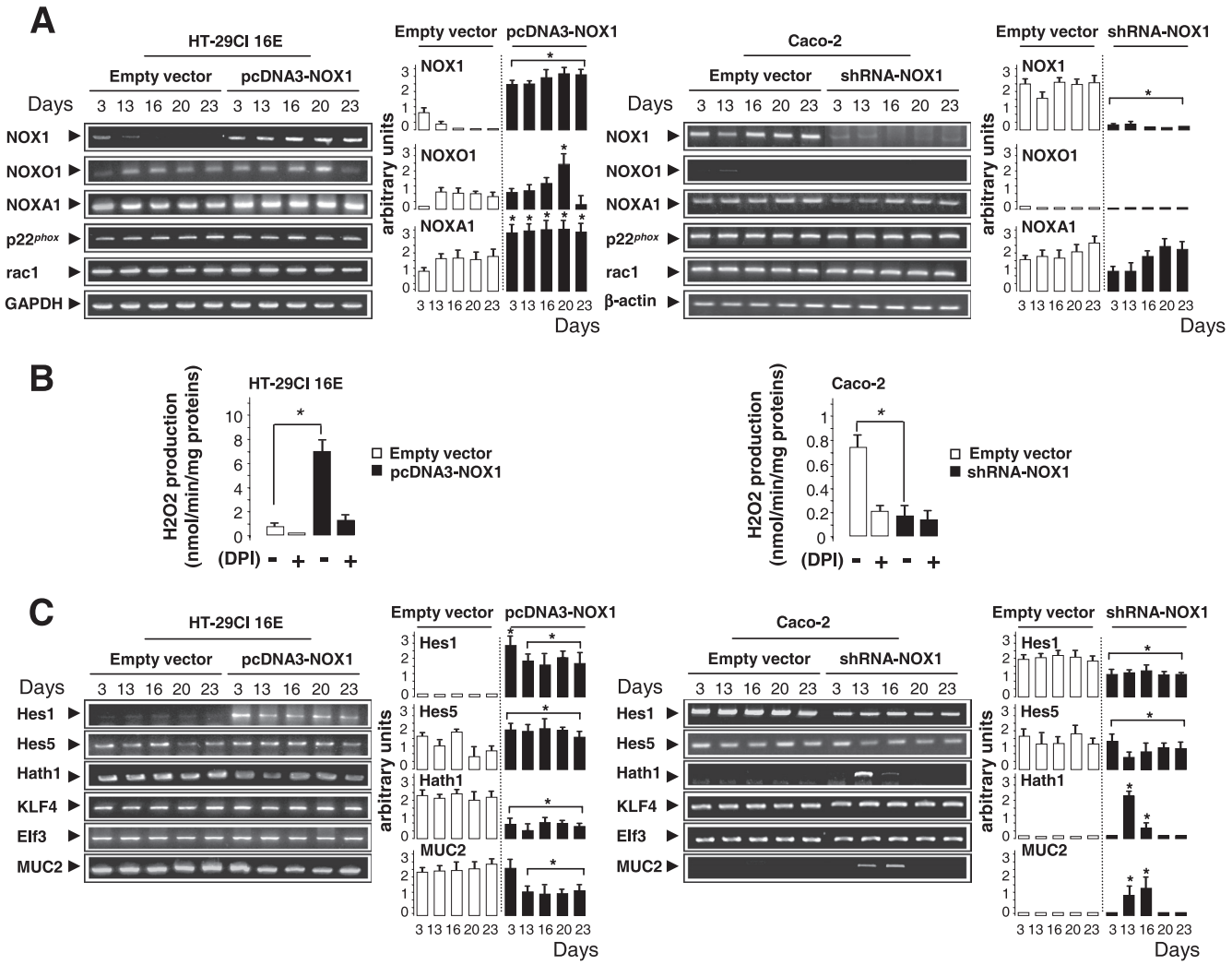


FIG. 3. Overexpression or silencing of NOX1 modulates the expression of transcription factors involved in cell lineage differentiation. HT-29Cl.16E and Caco-2 cells were transfected with pcDNA3-NOX1 or pEBV-shRNA-NOX1, respectively, or with the corresponding empty vectors. Semiquantitative RT-PCR analysis of *NOX1*, *NOXO1*, *NOXA1*, $p22^{phox}$, and *rac1* mRNA levels (A) or of transcription factors involved in cell fate (C) during cell proliferation (day 3) and differentiation (days 13 to 23) is shown. *GAPDH* and β-*actin* mRNA levels were used as controls for HT-29Cl.16E and Caco-2 cells, respectively. The ratio between each mRNA level and that for GAPDH or β-actin was quantified by scanning densitometry. Values are representative of 3 individual experiments performed in triplicate; means ± SEM are shown. *, $P < 0.001$ relative to empty vector. (B) PMA-induced ROS production in transfected HT-29Cl.16E and Caco-2 cells was measured by luminol-enhanced chemiluminescence in the presence or absence of DPI, an inhibitor of flavoproteins. Values are means ± SEM for three independent experiments. *, $P < 0.001$ relative to results with empty vector.

**Western blot analysis.** Colon tissue was homogenized in radioimmunoprecipitation assay (RIPA) buffer (50 mM Tris-Cl [pH 8.0], 320 mM sucrose, 0.1 mM EDTA, 1 mM dithiothreitol [DTT], 1% Nonidet P-40, 0.1% SDS, and 1% protease/phosphatase I and II inhibitor cocktail [Sigma]). Cells were rinsed, scraped off, collected, and sonicated in ice-cold phosphate-buffered saline (PBS) containing a cocktail of protease and phosphatase inhibitors. Proteins (50 to 100 μg) were separated by 10% SDS-PAGE, transferred using an iBlotGel transfer device (Invitrogen), and probed with primary antibodies: AKT, phospho-AKT, glycogen synthase kinase 3-β (GSK3β), phospho-GSK3α/β, PTEN, phospho-PTEN, β-catenin, phospho-β-catenin, p50, p65, phospho-p65, IκBα, phospho-IκBα, IκB kinase beta (IKKβ), phospho-IKKβ (Cell Signaling), E-cadherin (Santa Cruz,), and Notch1 intracellular domain (NICD). Horseradish peroxidase (HRP)-conjugated secondary antibodies were detected using ECL reagents (Pierce).

**Immunoprecipitation.** Immunoprecipitations (IPs) were performed with sh-NOX1 cells transfected with PTEN or scrambled siRNA or from scrapped colonic epithelium of wild-type (WT) and $NOX1^{KO}$ mice. Lysates were sonicated, centrifuged, and precleared with 75 μl protein G-Sepharose overnight at 4°C using an immunoprecipitation kit (GE Healthcare). Precleared supernatants were incubated with anti-β-catenin (2.5 μg/ml; Cell signaling) or anti-E-cadherin (2 μg/ml; Santa Cruz) antibodies for 2 h at 4°C and then with 50 μl protein G-Sepharose overnight at 4°C. Immunoprecipitates were rinsed twice in lysis buffers (Roche Diagnostics) according to the manufacturer's instructions. Sepharose-bound proteins were separated by 10% SDS-PAGE and transferred to nitrocellulose. The membranes were incubated with anti-β-catenin, anti-E-cadherin, anti-PTEN (Cell Signaling), or antiphosphotyrosine (Upstate) antibodies. Secondary antibodies HRP-conjugated anti-rabbit IgG (GE Healthcare) or rabbit IgG TrueBlot (eBioscience) were detected using ECL reagents.

**PTEN oxidation.** Colonic tissues from WT and $NOX1^{KO}$ mice were homogenized under nitrogen flux in chilled, nitrogen-saturated, thiol-free RIPA buffer containing 4 mg/ml iodoacetamide (Sigma). After nonreducing PAGE, reduced and oxidized forms of PTEN were detected by immunoblotting. When appropriate, β-mercaptoethanol was added before iodacetamide treatment.

**Histology, immunohistochemistry, and immunofluorescence assays.** Colons were flushed with cold PBS and fixed in 10% neutral-buffered formalin (Sigma) at 4°C. Paraffin-embedded sections (5 μm) were deparaffinized and stained with periodic acid-Schiff reagent and/or Alcian blue solution. BrdU was detected using anti-BrdU (Sigma). Immunohistochemistry was performed on sections heated for 10

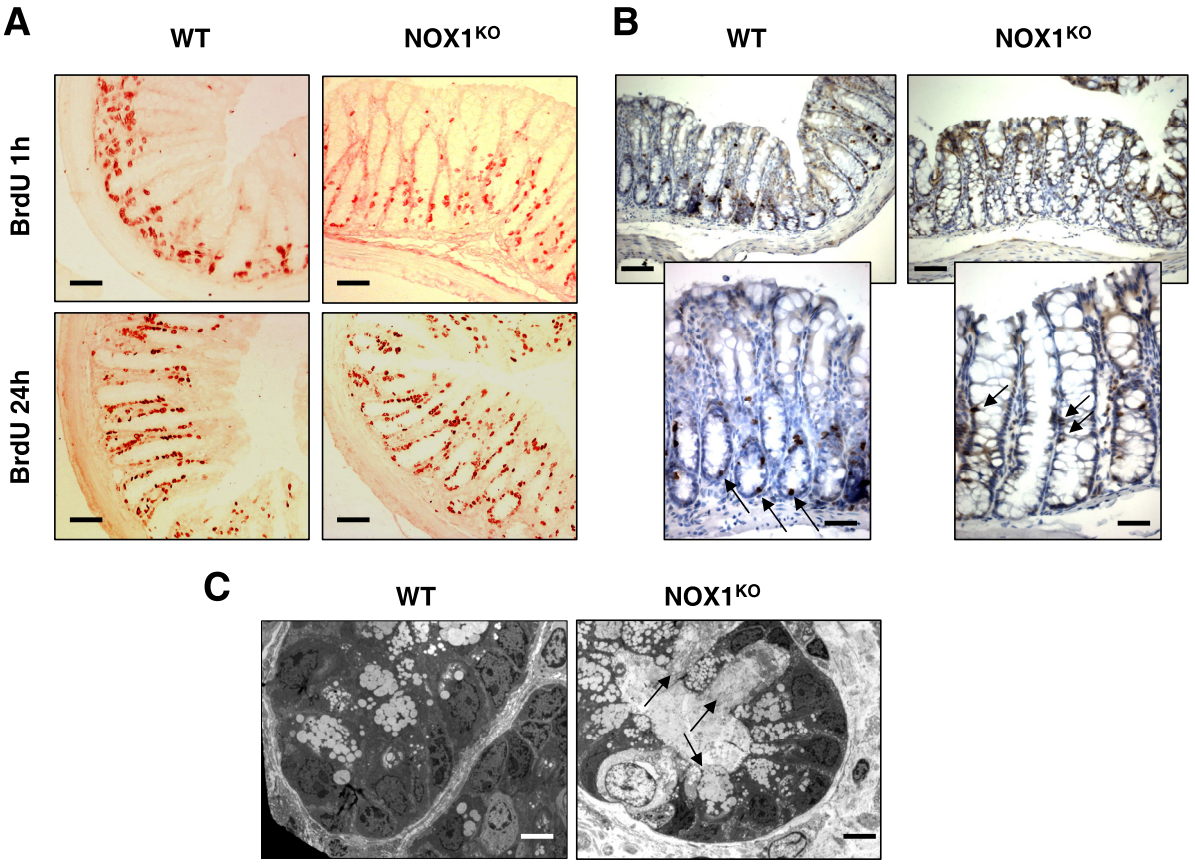


FIG. 4. NOX1 deficiency reduces the population of proliferating progenitors and modifies their spatial distribution. Immunohistochemical analysis of sections of distal colon from WT and $NOX1^{KO}$ mice stained with anti-BrdU antibody 1 h or 24 h after administration of BrdU (A) or with an antibody against the proliferating antigen phospho-histone 3 (B). (A) The number of BrdU-positive cells (red) 1 h after administration of BrdU is reduced in the colons of $NOX1^{KO}$ mice, and the proliferating cells, which are mostly confined to the bottom of the crypt domain in WT mice, are scattered along the first third of the crypt in $NOX1^{KO}$ mice. BrdU-positive cells migrated to the tops of crypts in $NOX1^{KO}$ mice 24 h after administration of BrdU, whereas they did not exceed two-thirds of the crypt length in WT mice (A). Scale bars, 80 μm. (B) Phospho-histone-3 staining (brown) confirms the decrease in the number of proliferating cells and their altered location in the crypt (arrows) in $NOX1^{KO}$ mice. Scale bar, 80 μm (top panels) or 50 μm (bottom panels). (C) Electron microscopy observation of colonic crypt sections reveals the presence of mature goblet cells (arrows) in an area of the crypt where proliferating cells normally reside. Scale bar, 5 μm.

min in 10 mM citrate buffer (pH 6.2) for antigen retrieval. After endogenous peroxidase removal (3% $H_2O_2$), sections were incubated with antibodies raised against Cdx1, Cdx2 (Biogenex), phospho-histone 3 (Upstate), or β-catenin (BD Transduction Lab). Secondary biotinylated anti-mouse or anti-rabbit antibodies (Vector Laboratories Inc.) were detected using the Vectastain ABC kit (Vector Laboratories Inc.). For immunofluorescence studies, sections were incubated in blocking buffer (PBS, 0.3% Triton X-100, and 20% goat serum) after antigen retrieval and then with anti-MUC2 (Santa Cruz), antivillin (Cell Signaling), anti-E-cadherin (BD-Biosciences), or anti-β-catenin (Cell Signaling) in 0.3% Triton in PBS, rinsed, and labeled with Alexa Fluor 546 goat anti-mouse IgG or Alexa Fluor 488 goat anti-rabbit IgG. Nuclei were stained using 4′,6-diamidino-2-phenylindole (DAPI) or TO-PRO-3 iodide (Invitrogen). Fluorescence was detected by confocal laser scanning microscopy (CLSM-510-META; Zeiss).

**ROS production assay.** ROS production was measured by the peroxidase-dependent luminol-enhanced chemiluminescence assay using Autolumat LB 953 (EG&G Berthold). Cells grown as confluent monolayers were collected by trypsinization and suspended in Hanks balanced salt solution ($10^6$ cells per 500 μl) containing a mixture of luminal (66 μM) and peroxidase (133 U/ml) (Sigma). After 10 min of preincubation, phorbol myristate acetate (PMA) (100 ng/ml) was added and measurements were performed for 30 min at 37°C. When used, diphenyleneiodonium (DPI) (2 μM) was added 10 min before measurement.

**Tissue preparation and short-circuit measurement.** Colons were rinsed in cold PBS, opened, and mounted in Ussing chambers. The tissues were bathed in carbogen-gassed Krebs-Ringer bicarbonate (KRB) (pH 7.4) solution on each side and kept at 37°C. Electrogenic ion transport was monitored continuously as short-circuit current. Potential difference in open circuit was also measured to calculate the total ionic conductance ($G$) (mS · $cm^2$). At steady state (~40 min), tissues were challenged mucosally with 10 mM butyrate. As an index of secretory response, tissues were further challenged with 100 μM carbachol.

**Electron microscopy.** Tissue samples from the distal colon were fixed in 3% glutaraldehyde in 0.1 M sodium cacodylate buffer (pH 7.2) for 24 h at 4°C, postfixed in osmium tetroxide, dehydrated with ethanol, and embedded in Epon. Ultrathin sections stained with lead citrate were examined on a Jeol 1010 electron microscope. Images were captured by a digital imaging system.

**Statistical analysis.** All results were expressed as means ± standard errors of the means (SEM). The Student $t$ test and one-way analysis of variance with a Tukey-Kramer multiple-comparison posttest were performed. Significance was set at a $P$ value of $<0.05$.

## RESULTS

**NOX1 deficiency affects epithelial lineage commitment in the colon.** To assess the role of NOX1 in the colon, we first examined the phenotype of epithelial cells in $NOX1^{KO}$ mice. Assessment of cell types revealed by periodic acid-Schiff/Alcian blue histochemistry, transmission electron microscopy, and immunofluorescence for MUC2 and villin demonstrated a significant 2-fold increase in the number of goblet cells at the

TABLE 2. Quantification of BrdU-positive cells in the distal colon sections of WT and NOX1$^{KO}$ mice[a]

| Time | No. of BrdU-positive cells/crypt in: | | Relative decrease (%) |
|---|---|---|---|
| | Wild-type mice | NOX1$^{KO}$ mice | |
| 1 h | 11.45 ± 2.15 | 7.83 ± 1.80* | ~30 |
| 24 h | 25.86 ± 5.30 | 24.12 ± 4.65 | ~7 |

[a] One hundred independent glands of 6 independent WT and NOX1$^{KO}$ mice were counted. Numbers of BrdU-positive cells per gland section after 1 h of BrdU correspond to poliferating crypt progenitor cells. After 24 h of BrdU, the leading edge of BrdU labeling marks the furthest extent of migration of progeny of precursor cells that have divided. *, $P < 0.01$ relative to control by Student's *t* test.

cost of colonocytes in NOX1$^{KO}$ mice compared with that for WT mice (Fig. 1). The number of enteroendocrine cells, the total number of cells per crypt, and the amount of apoptotic cells were similar in control and experimental models (data not shown). Consistent with very low *NOX1* mRNA levels in normal small intestine, no significant differences in the small intestinal phenotype were detected between WT and NOX1$^{KO}$ mice (data not shown). We next asked whether an increase in goblet cells changes colon physiology. Functional analysis of colonic mucosa in an Ussing chamber revealed an ~50% decrease in baseline short-circuit current (Isc) as an index of total ionic transports across the epithelium together with decreased chloride secretion in response to the cholinergic agonist carbachol in NOX1$^{KO}$ mice, consistent with the decrease in the number of colonocytes (Table 1). The response to butyrate challenge remained unchanged, suggesting no significant modification of sodium-associated absorption (Table 1). Accordingly, it should be noticed that body weights of WT and NOX1$^{KO}$ mice were similar, consistent with a functional adaptation of the absorptive function in mutant mice. In parallel, we found that *NOX1* mRNA expression was differentially regulated in different colon cancer cell lines that spontaneously differentiate into fully mature goblet or enterocyte-like cells (Fig. 2). A loss of *NOX1* mRNA occurred during the course of mucus-secreting differentiation of HT-29Cl.16E cells (Fig. 3A). Conversely, although *NOX1* mRNA expression levels decreased slightly during the exponential phase of growth of Caco-2 cells, its expression was reactivated during the course of enterocytic differentiation (Fig. 3A). Overexpression of NOX1 in HT-29Cl.16E cells or silencing of NOX1 in Caco-2 cells resulted in significant changes in ROS production (Fig. 3A and B) that were associated with modifications in expression of the basic helix-loop-helix transcription factors involved in cell fate determination, *Hes1-5* and *Math1* (Fig. 3C). mRNA expression

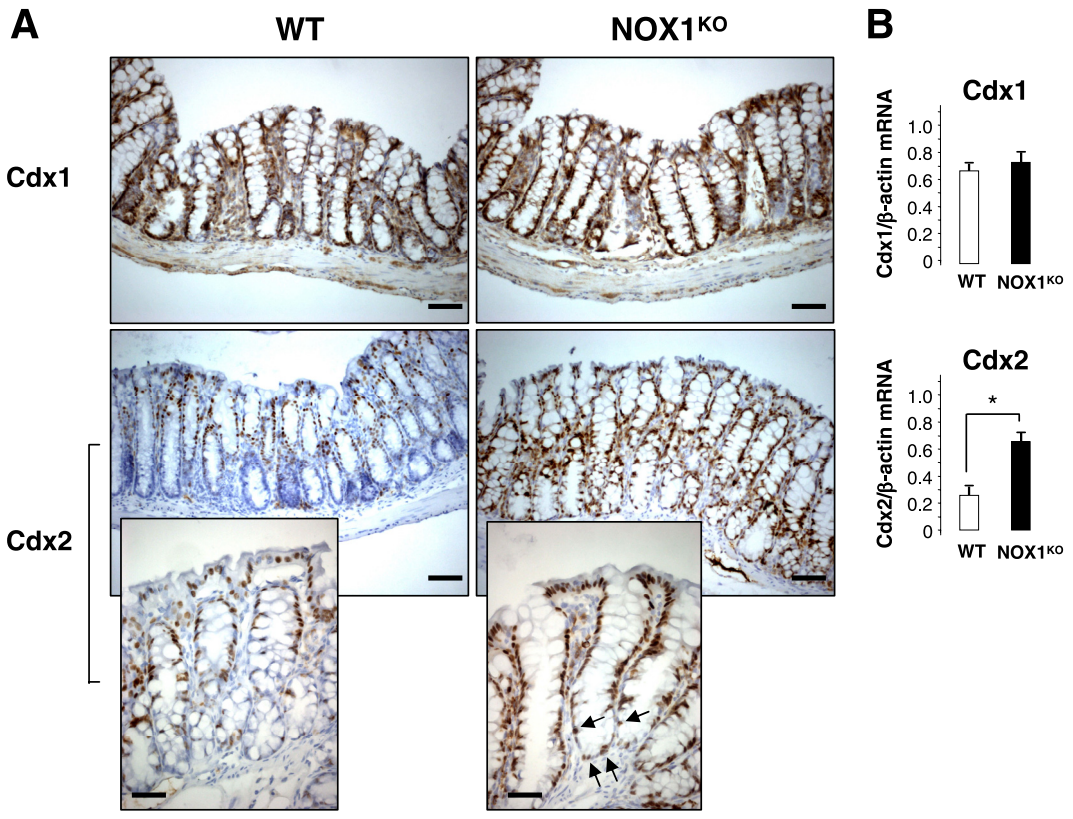


FIG. 5. Expression and localization of caudal-related homeobox Cdx proteins in the colon. (A) Immunohistological analysis of Cdx1 and Cdx2 in distal colon sections reveals similar staining for Cdx1 along the crypt (brown) in WT and NOX1$^{KO}$ mice; scale bar, 80 μm. In contrast, Cdx2 expression was upregulated in NOX1$^{KO}$ mice; scale bar, 80 μm. Magnification of the micrographs shows that nuclear staining of Cdx2 can be ectopically found at the bottom of the crypts in NOX1$^{KO}$ mice (arrows); scale bar, 50 μm. (B) RT-PCR from the colon reveals similar expression levels of *Cdx1* in both groups of mice and significantly increased levels of *Cdx2* in NOX1$^{KO}$ mice. *Cdx1*/β-*actin* and *Cdx2*/β-*actin* mRNAs were quantified by scanning densitometry. Values are representative of 2 individual experiments (means ± SEM); $n = 9$ for WT and NOX1$^{KO}$ mice. *, $P < 0.001$ relative to results for control (Student's *t* test).

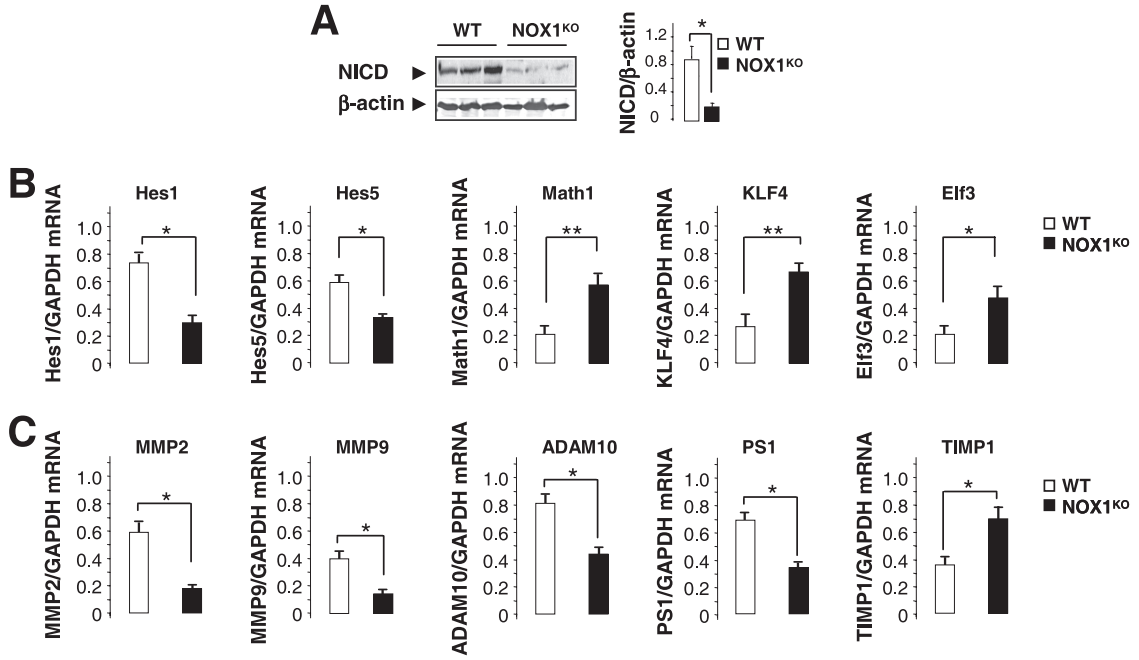


FIG. 6. NOX1 fine-tunes the activity of Notch1 signaling pathway. (A) Representative immunoblot analysis of NICD expression in colonic tissues from three individual WT and NOX1$^{KO}$ mice. β-Actin was used as a loading control. Note that NICD expression was severely depressed in NOX1$^{KO}$ mice compared to that in WT mice. NICD/β-actin was quantified by scanning densitometry. Data obtained in two independent experiments are expressed as means ± SEM; $n = 6$ for WT and NOX1$^{KO}$ mice; *, $P < 0.001$ relative to results for control (Student's $t$ test). (B) Semiquantitative RT-PCR from the colon shows decreased expression of *Hes1* and *Hes5* associated with derepression of *Math1*, *KLF4*, and *ElF3* transcription. Values are representative of two individual experiments, means ± SEM; $n = 9$ for WT and NOX1$^{KO}$ mice. *, $P < 0.001$ relative to results for control (Student's $t$ test). (C) Expression of γ-secretase (presenilin 1 [PS1]), proteases (matrix-metalloproteinases 2/9 [MMP2/9] and ADAM10), and TIMP1 (an inhibitor of MMPs) directly or indirectly involved in Notch1 activation, measured by semiquantitative RT-PCR for WT and NOX1$^{KO}$ mice. The *GAPDH* mRNA level was used as a loading control. The ratio between each mRNA level and *GAPDH* was quantified by scanning densitometry. Values are means ± SEM of two independent experiments ($n = 9$ for WT and NOX1$^{KO}$ mice); *, $P < 0.001$; **, $P < 0.0001$ (relative to results for control).

of two other transcription factors, Kruppel-like factor 4 (KLF4) and Elf3, known to be involved in the terminal differentiation of goblet cells, was depicted in Fig. 3C. Similarly, the *MUC2* expression level was inversely correlated with the presence of NOX1 (Fig. 3C).

Together, these results suggest that the majority of differentiated cells emerging from NOX1-deficient crypts adopt a secretory fate, consistent with the observation that the absence or presence of NOX1 in cultured colon cancer cells impacts the expression of goblet- or enterocyte-specific differentiation factors, respectively.

**NOX1 deficiency affects both proliferation and localization of progenitor cells in the colon.** Cellular homeostasis in NOX1$^{KO}$ crypts was next examined by observing crypt proliferation and migration of bromodeoxyuridine (BrdU)-labeled S-phase cells. The colons of NOX1$^{KO}$ mice sacrificed 1 h after BrdU exposure displayed a significant decrease in the number of BrdU-positive cells (Fig. 4A and Table 2) and an alteration in the spatial distribution of proliferating cells (Fig. 4A). This result was confirmed by staining colonic sections for phosphohistone 3, a mitosis-specific marker (Fig. 4B). Altogether, these data indicated that a lack of NOX1 perturbs cell cycle entry of progenitor cells and influences cell positioning in the crypts. This analysis was extended by examining the upward migration of cells that started to differentiate 24 h after BrdU exposure. The position of the leading edge of BrdU labeling, which marks the furthest extent of migration of progeny of precursor cells, was higher in NOX1$^{KO}$ mice than in WT mice (Fig. 4A), suggesting that NOX1 deficiency may promote a rapid conversion of progenitor cells into postmitotic goblet cells and/or a rapid migration of cells along the crypt axis. Electron microscopy revealed an expansion of the mature goblet cell population within the crypts in NOX1$^{KO}$ mice where progenitors normally undergo rapid division (Fig. 4C). Consistently, caudal-related homeobox *Cdx2* mRNA expression, a master regulator of intestinal cell identity that regulates goblet-specific *MUC2* and *Math1* gene expression (24, 37, 39), was strongly increased in NOX1$^{KO}$ mice, and nuclear staining for Cdx2 was ectopically expressed at the bottom of crypts in NOX1$^{KO}$ mice compared to that in WT mice (Fig. 5).

**NOX1 regulates Notch1 and Wnt/β-catenin signaling cascades.** Since the Wnt and Notch1 pathways are known to interplay in the regulation of intestinal epithelial cell proliferation and fate, we asked whether the phenotype observed in NOX1$^{KO}$ mice is linked to alterations in these signaling pathways. A large body of evidence suggests that Notch1 signaling regulates a binary decision between absorptive and secretory cell fates (8, 11, 61). Engagement of the Notch1 receptor by Notch ligands induces a two-step proteolytic cleavage that releases the Notch1 intracellular domain (NICD). NICD binds the transcriptional factor RBP-J (recombining binding protein suppressor of hairless) and stimulates *Hes1* and *Hes5* gene

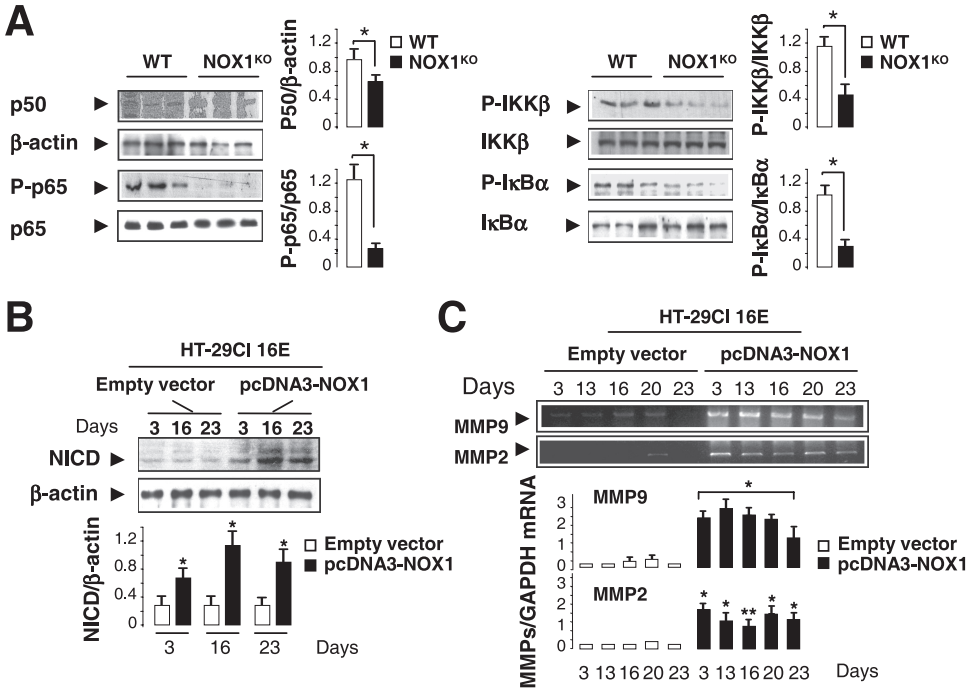


FIG. 7. NOX1 modulates NF-kB activation, MMP9/2 expression, and NICD production. (A) Assessment of NF-κB activity by Western blot analysis in WT and NOX1$^{KO}$ mice. β-Actin was used as a loading control. Values are means ± SEM of results for 3 mice per group. *, $P < 0.001$ relative to results for the control. (B) Western blot analysis of NICD in HT-29Cl.16E cells transfected with pcDNA3-NOX1 or empty vector in proliferating (day 3) or differentiated (days 16 and 23) cells. β-Actin was used as a loading control. Values are representative of 3 individual experiments performed in triplicate. (C) Expression of matrix-metalloproteinases 9/2 (MMP9 and -2) in HT-29Cl.16E cells transfected with pcDNA3-NOX1 or empty vector in proliferating (day 3) or differentiated (days 13 to 23) cells. The *GAPDH* mRNA level was used as a loading control. The ratio of each mRNA level to that for *GAPDH* was quantified by scanning densitometry. Values are representative of 3 individual experiments performed in triplicate (means ± SEM)l *, $P < 0.001$; **, $P < 0.005$ (relative to results with empty vector).

transcription and subsequent *Math1* repression in a Hes1-dependent manner (65), triggering absorptive determination. Consistent with the increase in goblet cell numbers, a functional downregulation of Notch1 signaling was observed in NOX1$^{KO}$ mice, as illustrated by dramatically reduced NICD expression (Fig. 6A), repressed levels of *Hes1* and *Hes5* transcription, and increased *Math1* mRNA expression (Fig. 6B). Furthermore, *KLF4* and *Elf3* mRNA levels were upregulated in the colons of NOX1$^{KO}$ mice compared with levels in WT mice (Fig. 6B). The phenotype that we observe is reminiscent of that of Hes1 or RBP-J knockout mice (20, 61). In contrast, Math1-deficient mice (65) or mice with forced expression of NICD (11), which lack goblet cells, show a phenotype opposite to that in NOX1$^{KO}$ mice. The gain-of-function phenotype described here suggests that NOX1 targets Notch1 signaling to control the lineage of progenitor cells. Although the mechanisms of NOX1-mediated Notch1 activation remain elusive, we show that mRNA expression levels of γ-secretase and of metalloproteinases (MMPs) involved in Notch1 activation were significantly reduced in NOX1$^{KO}$ mice (Fig. 6C). Given that ROS play a major role in the NF-κB-dependent expression of metalloproteases (34) and that Notch1 augments NF-κB activity (55), we demonstrated that basal NF-κB activation is affected in the colons of NOX1$^{KO}$ mice, as illustrated by differential phosphorylation of p65, IKKβ, and IκBα (Fig. 7A). Furthermore, overexpression of NOX1 in HT-29Cl.16E cells reactivated NICD and *MMP9/2* expression levels (Fig. 7B and C), consistent with up- and downregulation of *Hes1* and *Hath1* (the human homolog of *Math1*) levels, respectively (Fig. 3C).

The Wnt cascade has been shown to affect cell fate determination via effects on progenitor cell proliferation (25, 43, 51). Consistently, inactivation of transcription factor 4 (encoded by *Tcf4*) or β-catenin (two downstream mediators of Wnt signals) or forced expression of the diffusible Wnt inhibitor, dickkopf homologue 1 (DKK1), leads to the loss of the proliferative compartment (for a review, see reference 44). As a result of a Wnt signaling defect, secretory cells seem to be lost when the Notch cascade remains active (25, 43). To investigate if active Wnt signaling is altered in the colons of NOX1$^{KO}$ mice, we assessed both the localization and transcriptional activity of β-catenin/Tcf4, which constitute the dominant switch between proliferating progenitors and differentiated cells. Using confocal microscopy and immunohistochemistry experiments, we observed a spatial β-catenin expression gradient along the crypt-to-cuff axis, and nuclear β-catenin was restricted to a subset of crypt cells in WT mice (Fig. 8A). In contrast, NOX1 deficiency enhanced both the β-catenin–E-cadherin complex level at the plasma membrane in the lower crypts (Fig. 8A) and Ser/Thr phosphorylation of β-catenin (Fig. 8B). Consistent with reduced Wnt/β-catenin/Tcf4 signaling activity, *c-Myc* and *cyclin D1* transcription was downregulated in the colons of NOX1$^{KO}$ *mice* (Fig. 8C). Rather than regulating gene transcription after nuclear translocation, β-catenin is driven to the E-cadherin complex to modulate cell-cell

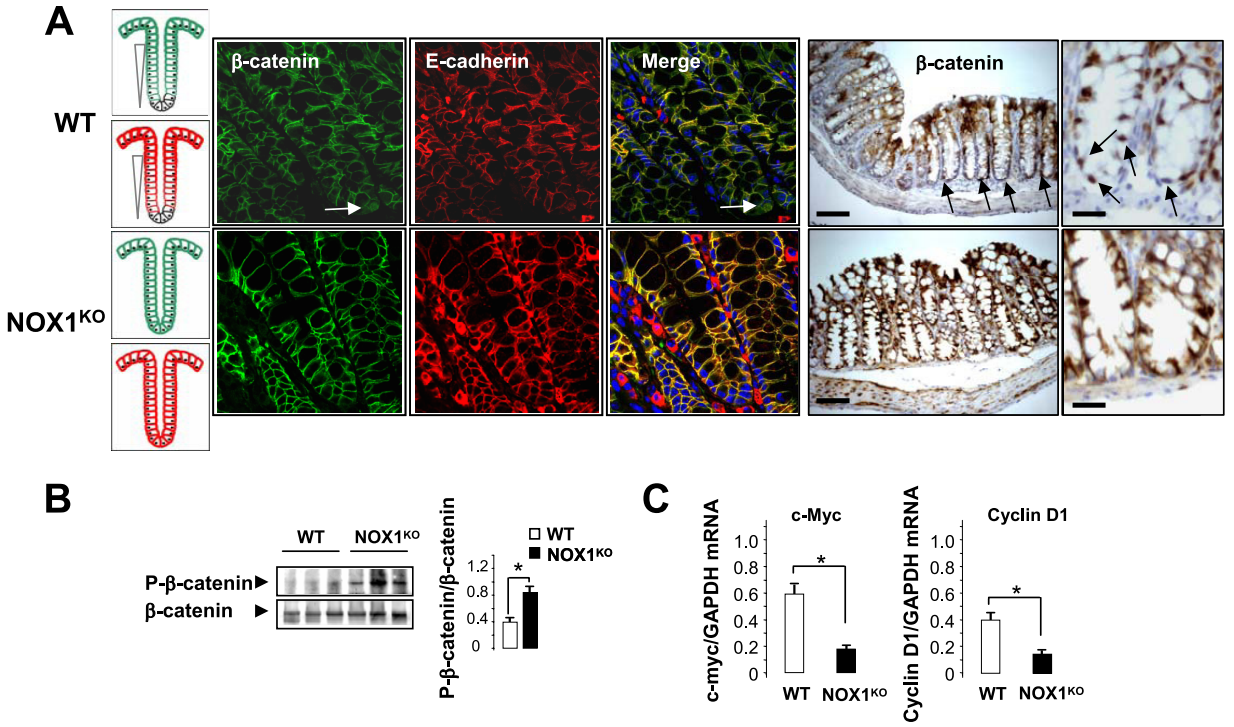


FIG. 8. NOX1 deficiency attenuates Wnt/β-catenin signaling pathway. (A) Immunofluorescence of colon sections using anti-β-catenin (green) and anti-E-cadherin (red) reveals that β-catenin associated with the plasma membrane as part of the β-catenin–E-cadherin complex was essentially detected at the upper part of the crypts in WT mice whereas this complex was also present at the bottom of the crypts in NOX1$^{KO}$ mice. Original magnification, ×60. The illustration in the left-hand micrograph schematizes the distribution of membrane β-catenin and E-cadherin in colonic crypt regions. Immunohistochemistry of colon sections using anti-β-catenin shows that nuclear β-catenin staining (brown) can be observed in many cells at basal positions of colon crypts only in WT mice (arrows). Scale bars, 80 μm or 50 μm. (B) Representative immunoblot analysis of phospho-β-catenin expression in colonic tissues from three individual WT and NOX1$^{KO}$ mice. Phospho-β-catenin (Ser$^{33/37}$/Thr$^{41}$)/β-catenin was quantified by scanning densitometry. Data obtained in two independent experiments are expressed as means ± SEM; $n = 6$ for WT and NOX1$^{KO}$ mice; *, $P < 0.001$ relative to results for the control (Student's $t$ test). (C) Accordingly, *c-Myc* and *Cyclin D1* transcription was repressed in NOX1$^{KO}$ mice. Values are representative of 2 individual experiments (means ± SEM); $n = 9$ for WT and NOX1$^{KO}$ mice. *, $P < 0.001$ relative to results for control (Student's $t$ test).

adherens junctions, cell cycle arrest, and differentiation in the NOX1$^{KO}$ crypts. Together, these results suggest that progenitor cells are arrested early in the cell cycle and forced to differentiate into goblet cells as a result of attenuated Wnt/β-catenin and Notch1 signaling in NOX1$^{KO}$ mice.

**NOX1 activates Wnt/β-catenin signaling in part through ROS-mediated PTEN inactivation.** Cross talk between the Wnt and Notch1 signaling pathways is likely to occur via the phosphatidylinositol 3-kinase (PI3K) cascade through AKT-mediated inactivation of GSK3β (10, 33). In support of this, inhibition of GSK3β-mediated β-catenin phosphorylation is the major mechanism that Wnt signals use to prevent β-catenin degradation. Furthermore, PI3K and GSK3β have both been identified as binding partners for NICD and as components of the Notch signaling pathway in lateral inhibition in *Drosophila melanogaster* (47). To gain insights into the function of PI3K/AKT/GSK3 signaling in regulating both of the Wnt and Notch1 signaling cascades, we analyzed the phosphorylation status of both AKT and GSK3 in the colons of WT and NOX1$^{KO}$ mice. We demonstrated that activation/dephosphorylation of GSK3 is dramatically increased in NOX1$^{KO}$ mice with a concomitant dephosphorylation of AKT at both Ser$^{473}$ and Thr$^{308}$ residues (Fig. 9A and B). We further examined activation of the tumor suppressor PTEN, a dual-specificity phosphatase which antagonizes PI3K/AKT signaling and acts in transit-amplifying cells as a negative regulator of the cell cycle (18). Previous reports have demonstrated that PTEN activity could be regulated at the level of transcription, through phosphorylation-dependent modulation of protein stability and/or through reversible oxidation (26, 58, 63). Although the level of PTEN transcription was unchanged between WT and NOX1$^{KO}$ mice, we demonstrated that phosphorylation of PTEN (Ser$^{380}$) was strongly reduced in NOX1$^{KO}$ mice (Fig. 9C), suggesting that ROS generated by NOX1 may indirectly modulate PTEN activity by activating intermediate redox-sensitive protein kinases. In addition, oxidation of the active-site Cys$^{124}$ residue by ROS, which negatively regulates PTEN activity (29, 30), was investigated. We reported that the percentage of the active form of PTEN (reduced form) was 30 to 35% higher in NOX1$^{KO}$ mice than in WT mice (Fig. 9D). Altogether, these results demonstrated that NOX1 deficiency enhanced PTEN activation by regulating both its oxidation and phosphorylation states. In order to ascertain the implication of PI3K/PTEN/AKT signaling in the phenotype observed in NOX1$^{KO}$ mice, forced PI3K/AKT activation was achieved by successive subcutaneous injections of recombinant insulin growth factor 1 (IGF1) for 4 days. The efficiency of IGF1 treatment was attested by dramatic enhancement of AKT

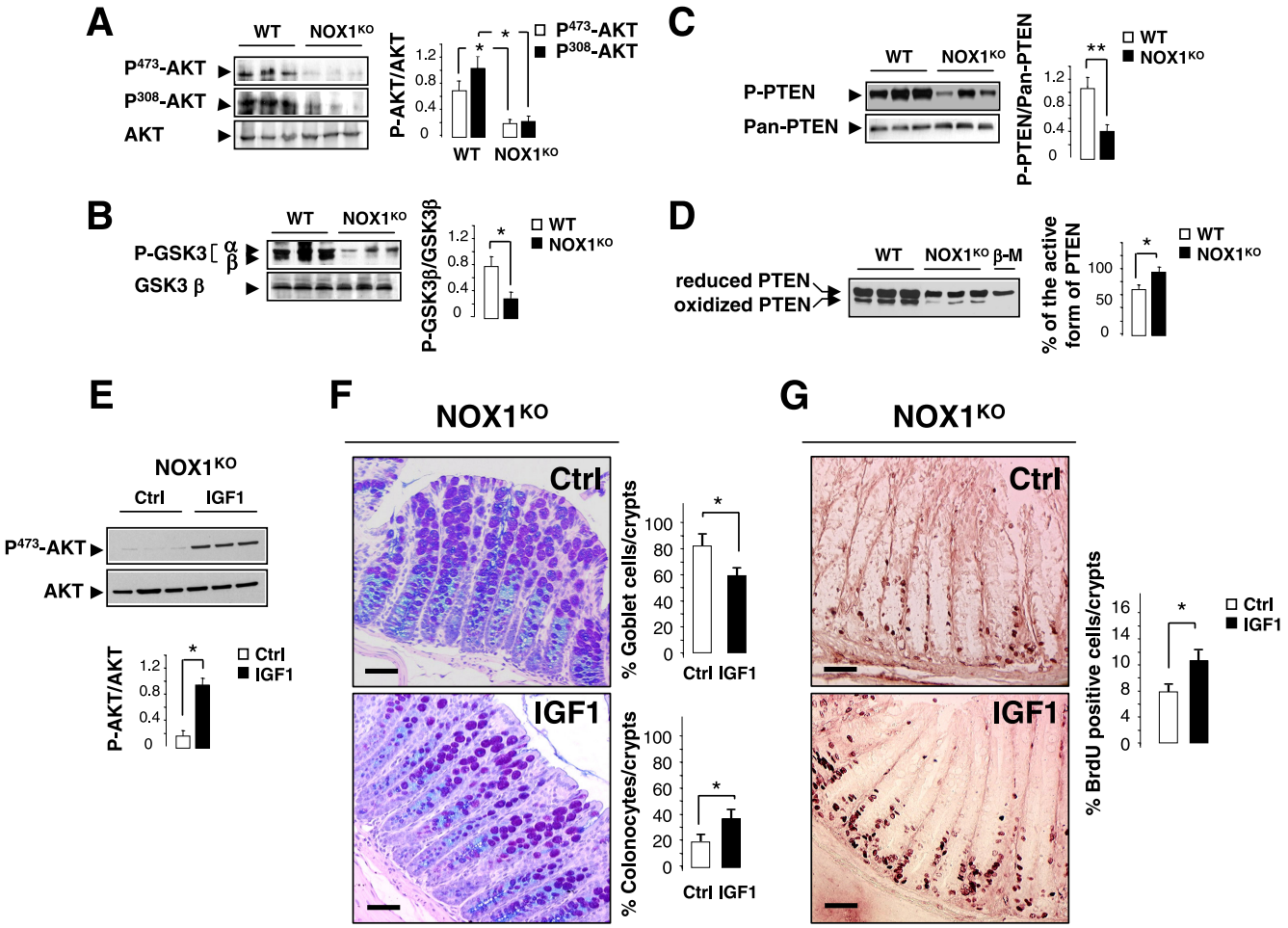


FIG. 9. Effect of NOX1 on goblet cell differentiation and cell proliferation implicates PTEN/AKT signaling cascade. Representative immunoblot analysis of phospho-AKT (A), phospho-GSK3 (B), or phospho-PTEN (C) expression in colonic tissues from three individual WT and NOX1$^{KO}$ mice. Phospho-AKT (Ser$^{473}$)/AKT and phospho-AKT (Thr$^{308}$)/AKT (A), phospho-GSK3α (Ser$^{21}$)/GSK3α and phospho-GSK3β (Ser$^{9}$)/GSK3β (B), and phospho-PTEN (Ser$^{380}$)/pan-PTEN (C) were quantified by scanning densitometry. Data obtained in two independent experiments are expressed as means ± SEM; $n = 9$ for WT and NOX1$^{KO}$ mice; ⁎, $P < 0.001$; ⁎⁎, $P < 0.05$ relative to results for the control (Student's $t$ test). (D) Detection of active (reduced) and inactive (oxidized) forms of PTEN on the basis of an electrophoretic mobility shift. Colonic crypt extracts from WT and NOX1$^{KO}$ mice were subjected to alkylation in the presence or absence of β-mercaptoethanol (β-M) and fractionated by nonreducing SDS/PAGE. The percentage of the active form of PTEN was determined by scanning densitometry. Data obtained in two independent experiments are expressed as means ± SEM; $n = 6$ for WT and NOX1$^{KO}$ mice; ⁎, $P < 0.0001$ relative to results for the control (Student's $t$ test). (E) Representative immunoblot analysis of Phospho-AKT (Ser$^{473}$)/AKT expression in colonic tissues from three individual NOX1$^{KO}$ mice treated twice daily with 2 μg/g Long-Arg$^{3}$-IGF1 (IGF1) for 4 days or with vehicle (HCl, 2 mM in PBS). Phospho-AKT/AKT was quantified by scanning densitometry. Data are expressed as means ± SEM; $n = 3$ for untreated and IGF1-treated NOX1$^{KO}$ mice; ⁎, $P < 0.001$ relative to results for the control (Student's $t$ test). (F) Representative sections of distal colon from NOX1$^{KO}$ mice treated (IGF1) or not (Ctrl) with IGF1 stained with periodic acid-Schiff and Alcian blue. Eight crypts per section with 2 individual sections from each animal were counted. Percentages of goblet cells and colonocytes per crypt are represented as means ± SEM ($n = 3$ for untreated and IGF1-treated NOX1$^{KO}$ mice); ⁎, significantly different from Ctrl ($P < 0.001$) (Student's $t$ test). (G) Immunohistochemical analysis of sections of distal colon from NOX1$^{KO}$ mice treated (IGF1) or not (Ctrl) with IGF1 stained with anti-BrdU antibody 1 h after administration of BrdU. The number of BrdU-positive cells per gland section was reported as detailed in Materials and Methods. ⁎, $P < 0.01$ relative to results for Ctrl (Student's $t$ test). Scale bars, 80 μm.

phosphorylation (Ser$^{473}$) (Fig. 9E). Interestingly, IGF1-dependent activation of the PI3K/AKT signaling pathway in part reduced the number of goblet cells by 30% (Fig. 9F) and increased cell proliferation by 35% (Fig. 9G) in the colons of NOX1$^{KO}$ mice. It is noteworthy that spatial distribution of progenitors at the bottom of the crypt was partly rescued by IGF1 treatment (Fig. 9G), suggesting an important role of the PI3K/PTEN/AKT signaling cascade in crypt localization, proliferation, and commitment of progenitor cells in the colon. Altogether, these results suggest that ROS generated by NOX1 may activate the Notch1 and Wnt/β-catenin signaling pathways in part through activation of the PI3K/AKT signaling cascade.

Several lines of evidence suggest that PTEN interacts indirectly with β-catenin by binding scaffolding proteins such as cadherins and thus participates in regulating adherens junctions and cell-cell adhesion (26, 58, 63). Since PTEN has been shown to be involved in E-cadherin–β-catenin complex assembly by reducing tyrosine phosphorylation of both proteins (2, 63), we assumed that increased PTEN activity in NOX1$^{KO}$

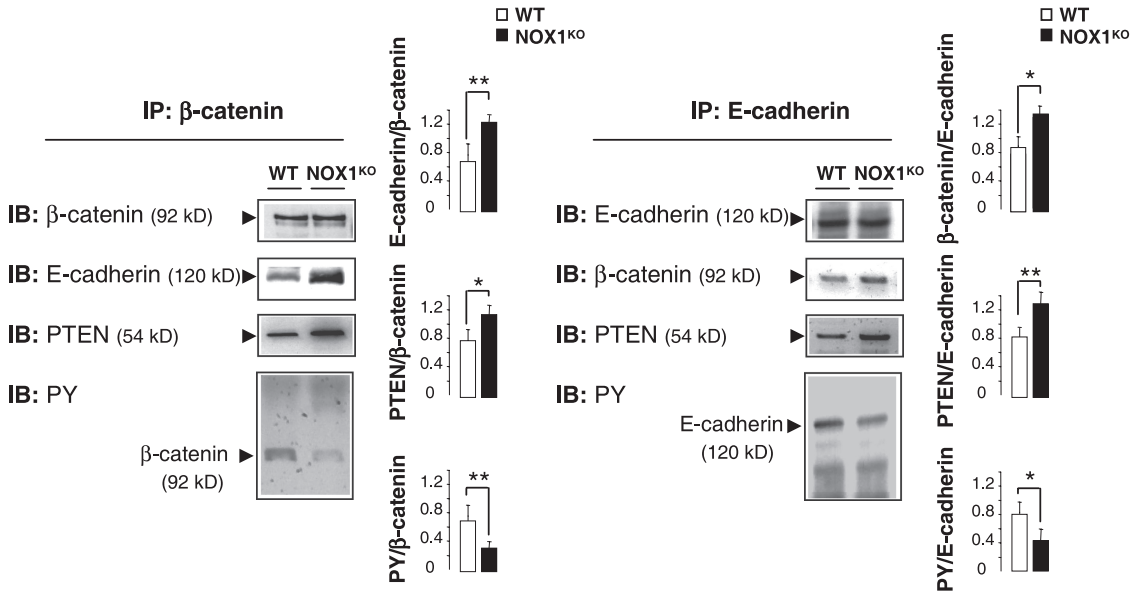


FIG. 10. PTEN activation facilitates β-catenin/E-cadherin association in NOX1$^{KO}$ mice. Colonic crypt lysates from WT and NOX1$^{KO}$ mice were subjected to immunoprecipitation (IP) with anti-β-catenin or E-cadherin antibodies. The IP material was then subjected to immunoblot analysis (IB) with antibodies recognizing β-catenin, E-cadherin, PTEN, or phosphotyrosine (PY). Data are means ± SEM; $n = 3$ for WT and NOX1$^{KO}$ mice; *, $P < 0.005$; **, $P < 0.001$ relative to results for control.

mice may be partially responsible for the more prominent localization of β-catenin to the cell surface. Accordingly, immunoprecipitation study demonstrates that association of PTEN with the E-cadherin–β-catenin complexes was increased in NOX1$^{KO}$ mice (Fig. 10). This association was accompanied by a reduction of tyrosine phosphorylation of both β-catenin and E-cadherin, which triggers the complex formation as a prerequisite for cell differentiation (Fig. 10). Consistently, E-cadherin–β-catenin complexes were more prominent in NOX1$^{KO}$ mice (Fig. 10), and silencing of PTEN by siRNA in short-hairpin *NOX1* RNA-transfected Caco-2 cells (Fig. 11A and B) restored tyrosine phosphorylation of β-catenin and E-cadherin and impaired their association with the cell surface (Fig. 11C). Collectively, these data show that NOX1 deficiency reduces tyrosine phosphorylation and triggers cellular redistribution of E-cadherin–β-catenin complexes by a PTEN-dependent mechanism, suggesting that NOX1 may play a role in activating progenitor cell self-renewal by regulating PTEN activity.

## DISCUSSION

Here we have shown that NOX1 may regulate the balance between cell proliferation and differentiation by modulating the PI3K/AKT, Wnt/β-catenin, and Notch1 signaling cascades in a ROS-dependent manner. As a result, NOX1-deficiency (i) perturbs cell cycle entry of progenitor cells and influences cell positioning in the crypts and (ii) promotes a rapid conversion of progenitor cells into postmitotic goblet cells at the expense of colonocytes. These findings support that NOX1 signaling is essential within the crypt compartment to maintain the undifferentiated state of the crypt progenitors and likely acts on a proximal step in cell type specification of the transit-amplifying precursor cells by coordinately controlling both Wnt and Notch1 signals.

The first evidence that Notch1 signaling plays a role in cell specification was previously reported in loss-of-function studies of Hes1 (20) and of its downstream target Math1 (65). It was shown that the choice between absorptive and secretory fates might be the first decision made by each progenitor cell and that Hes1 and Math1 play opposite roles in this decision making. Moreover, inhibition of Notch1 activation using pharmacological approaches or genetic manipulation results in the predominance of the goblet cell lineage in the gastrointestinal tract (14, 38, 61), reminiscent of the goblet cell morphology seen in the colons of NOX1$^{KO}$ mice. Conversely, conditional expression of NICD in the intestine inhibits differentiation of crypt progenitor cells, resulting in a large increase in undifferentiated transit-amplifying cells associated with a lack of goblet cells (8, 11, 61). One potential mechanism by which NOX1 may regulate the cell fate decision of progenitors is through proteolytic activation of Notch1. Although the mechanisms by which NOX1 induces Notch1 activation remain to be fully characterized, both our *in vitro* and *in vivo* data demonstrate that NICD expression levels and subsequent *Hes1* and *Math1* levels strongly correlate with NOX1 expression and cell fate determination. Furthermore, indirect support for the role of NOX1 in the proteolytic processing of Notch1 stems from the downregulation of proteases observed in NOX1$^{KO}$ mice. In support of this, it has been recently shown that MMP9$^{-/-}$ mice exhibit an increase in goblet cells with a concomitant decrease in colonocytes by downregulation of the proteolytic activation of Notch1 (14, 38, 61). Moreover, activation of the NADPH oxidase homolog dual oxidase 1 (DUOX1) within the human airway epithelium has been shown to activate the tumor necrosis factor alpha (TNF-α) converting enzyme TACE/

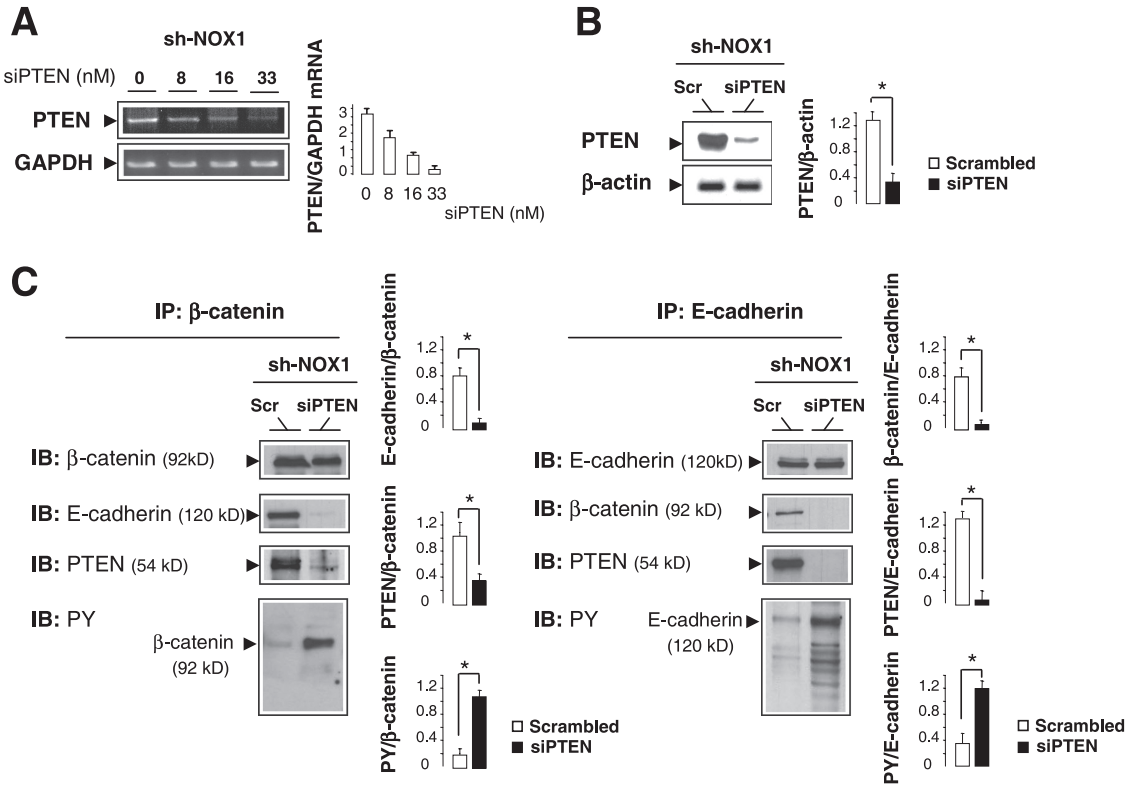


FIG. 11. Silencing of PTEN impairs β-catenin–E-cadherin complex formation in sh-*NOX1* RNA-transfected Caco-2 cells. (A) Semiquantitative RT-PCR shows the expression of *PTEN* in stably transfected Caco-2 cells with the sh-*NOX1* RNA construct (sh-NOX1) treated with increased concentrations of *PTEN* siRNA (siPTEN). the *GAPDH* mRNA level was used as a loading control. The ratio between *PTEN* and *GAPDH* mRNA levels was quantified by scanning densitometry. Values are representative of two individual experiments performed in triplicate. (B) The efficiency of PTEN siRNA was confirmed by Western blotting in sh-NOX1 Caco-2 cells transfected with siPTEN or scrambled (Scr) siRNA. β-Actin served as the loading control. PTEN/β-actin was quantified by scanning densitometry. Values are representative of two individual experiments performed in triplicate. *, $P < 0.001$ relative to results for scrambled siRNA. (C) Cell lysates from sh-NOX1 Caco-2 cells transfected with siPTEN or scrambled (Scr) siRNA were subjected to immunoprecipitation (IP) with anti-β-catenin or anti-E-cadherin antibodies. The IP material was then subjected to immunoblot analysis (IB) with antibodies recognizing β-catenin, E-cadherin, PTEN, or phosphotyrosine (PY). Values are representative of two individual experiments performed in triplicate. *, $P < 0.001$ relative to results for scrambled siRNA.

ADAM17 by an $H_2O_2$-dependent mechanism (52, 53), suggesting that ROS may directly regulate protease activity.

A large body of evidence indicates the presence of hierarchical regulation between the Wnt/β-catenin and Notch1 cascades for balancing intestinal proliferation/differentiation (11, 40, 49, 61). Here we have revealed that the regulatory circuit linking NOX1-mediated ROS production with the Wnt/β-catenin and Notch1 pathways is required for maintaining crypt cells in a proliferative state. This is achieved, at least in part, by simultaneously enhancing β-catenin transcriptional activity, cellular redistribution of E-cadherin–β-catenin complexes through ROS-dependent PTEN inactivation, and Notch1 signaling activity in the stem cell niche (Fig. 12). We propose that NOX1 may partially govern cell activation and proliferation and the number of progenitor crypt cells by cooperating with the Wnt and PI3K/AKT pathways to control nuclear localization of β-catenin and hence the regulation of β-catenin targets, such as cyclin D1 and c-Myc. The interplay between Wnt and PI3K/AKT is a subject of debate. A genetic experiment has demonstrated that removal of the two inhibitory serine residues ($Ser^{9/21}$) in GSK3 knock-in mice has no effect on Wnt signaling (36). These findings suggest that there are at least two pools of GSK3 in cells, one associated with Axin and refractory to phosphorylation by AKT at $Ser^{9/21}$ and another that can be regulated by AKT (for a review, see reference 64). However, several groups have proposed that Wnt and AKT induce phosphorylation of GSK3 isoforms at the same sites (3, 12, 66). In our study, the importance of the PI3K/AKT signaling pathway in progenitor proliferation and differentiation has been outlined by activating the insulin pathway by recombinant IGF1 in $NOX1^{ko}$ mice. Consequently, we propose that direct or indirect redox modulation of the PI3K/AKT and Wnt signaling pathways results in phosphorylation/inhibition of GSK3β and translocation of β-catenin in the nucleus as well as Notch1 activation. Consistent with this hypothesis, we show that loss of NOX1 results in increased PTEN activity due to the combination of significantly reduced phosphorylation and oxidation levels that could in part account for the profound effects on the reduction in active AKT. It is not excluded that the downregulation of PI3K/AKT signaling may also be achieved by the inactivation of other redox-sensitive kinases, such as PDK1 and Src (7). On the other hand, even if other phosphatases may also be concerned (54), it is noteworthy that ROS-dependent PTEN inactivation is essential to increase tyrosine phosphory-

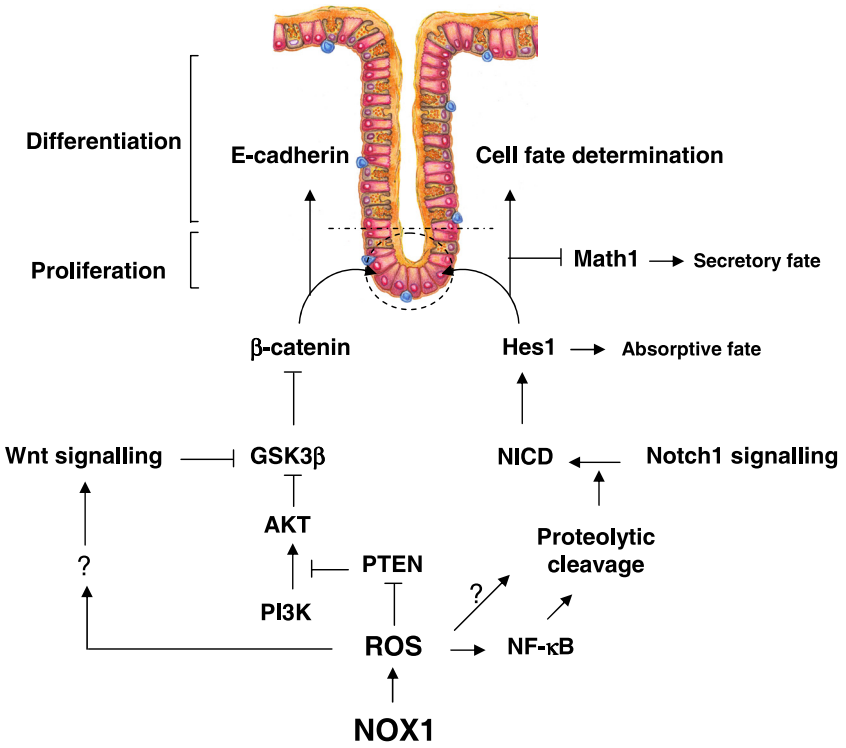


FIG. 12. Schematic representation of NOX1-induced regulatory networks controlling progenitor cell fate in the colon.

lation of E-cadherin and β-catenin and to disassemble E-cadherin/β-catenin complexes, events that lead to an increase in the transcriptional activity of β-catenin (2, 63).

The role of PTEN in intestinal homeostasis is controversial even in studies using similar experimental models. Marsh et al. (35) reported that specific deletion of *Pten* within the epithelium of two intestinal Cre recombinase models has no adverse effect on proliferation, crypt progenitor phenotype, or the Wnt signaling pathway, suggesting that PTEN is redundant in intestinal epithelium. In contrast with this prediction, Langlois et al. (27) recently showed that a conditional loss of epithelial *Pten* leads to an intestinomegaly associated with an increase in epithelial cell proliferation, suggesting a role for PTEN in the commitment of the multipotential-secretory precursor cell. Nonetheless, a loss of epithelial *Pten* did not result in increased nuclear β-catenin protein levels, nor was it sufficient to promote tumorigenesis initiation except in the context of activated Wnt signaling (27, 35). In contrast, previous studies showed that PTEN acts as a negative regulator of the cell cycle in intestinal stem cells and helps govern stem cell activation by helping control nuclear localization of β-catenin (17, 18, 42). Therefore, future experiments with an $NOX1^{KO}$/villin Cre-$Pten^{fl/fl}$ mouse model would help to demonstrate that PTEN is or is not a key target of NOX1 functions in controlling the relationship between PI3K/AKT, Wnt and Notch signaling, and the fate of colonic epithelial progenitors.

Of interest, it was shown that Notch signaling and the PI3K-AKT pathways synergize *in vivo* in a *Drosophila melanogaster* model of Notch-induced tumorigenesis and that mutational loss of *PTEN* is associated with the resistance of human T-cell lymphoblastic leukemias and lymphomas to pharmacological inhibition of Notch1 (41), suggesting that PTEN might be functionally linked to Notch1 signaling. Furthermore, hyperactivated PI3K/AKT signaling leads to upregulation of Notch1 through NF-κB activity in melanoma development (6), suggesting an overt link between the Notch1 and PI3K/AKT signaling pathways. In this context, our results warrant further studies to test this interplay in the colon homeostasis.

A wealth of evidence indicates that the Wnt/β-catenin, Notch1, and PI3K/AKT cascades might be the major driving force behind the proliferative potential of neoplastic cells. Because the overexpression of NOX1 is often detected in precancerous and well-differentiated adenocarcinomas (13), the present data indicate that NOX1 might coordinately drive oncogenic potential. NOX1 modulation therefore might represent a novel strategy for colorectal cancer.

## ACKNOWLEDGMENTS

We thank R. Kopan (Washington University), F. Logeat, and D. Ndiaye (Institut Pasteur, Paris, France) for the Notch construct and antibodies against Notch1 and NICD; S. H. E. Moore (CRB3 INSERM, Paris, France) for discussion and critical reading of the manuscript; T. L. Leto (NIH, Bethesda, MD) for the gift of the pcDNA3-NOX1 construct; C. Bonhomme (Strasbourg, France) for the gift of Cdx1 antibody; and S. Benadda and O. Thibaudeau (IFR02, Paris, France) for technical help.

Financial support was from the Institut National de la Santé et de la Recherche Médicale (INSERM), Association François Aupetit (AFA) (to E.O.D.), Assistance Publique-Hôpitaux de Paris (AP-HP) (Interface Fellowship to E.O.D.), Société Nationale Française de Gastro-Entérologie (SNFGE), Association Française pour l'Étude du Foie (AFEF), and Programme National de Recherche en Hépato-Gastroentérologie (PNRHGE) (to X.T. and E.O.D.). N.C. was supported by a Ph.D. student's grant from the AFA. S.B.M. was supported by a Ph.D. student's grant from the Ligue Nationale contre le Cancer. C.G. was supported by

a postdoctoral fellowship from EASL. X.T. was supported by a doctoral position from INSERM (poste d'accueil).

## REFERENCES


1. **Arbiser, J. L., J. Petros, R. Klafter, B. Govindajaran, E. R. McLaughlin, L. F. Brown, C. Cohen, M. Moses, S. Kilroy, R. S. Arnold, and J. D. Lambeth.** 2002. Reactive oxygen generated by Nox1 triggers the angiogenic switch. Proc. Natl. Acad. Sci. U. S. A. **99:**715–720.
2. **Barbieri, S. S., L. Ruggiero, E. Tremoli, and B. B. Weksler.** 2008. Suppressing PTEN activity by tobacco smoke plus interleukin-1beta modulates dissociation of VE-cadherin/beta-catenin complexes in endothelium. Arterioscler. Thromb. Vasc. Biol. **28:**732–738.
3. **Baryawno, N., B. Sveinbjornsson, S. Eksborg, C. S. Chen, P. Kogner, and J. I. Johnsen.** 2010. Small-molecule inhibitors of phosphatidylinositol 3-kinase/Akt signaling inhibit Wnt/beta-catenin pathway cross-talk and suppress medulloblastoma growth. Cancer Res. **70:**266–276.
4. **Bates, M. D., C. R. Erwin, L. P. Sanford, D. Wiginton, J. A. Bezerra, L. C. Schatzman, A. G. Jegga, C. Ley-Ebert, S. S. Williams, K. A. Steinbrecher, B. W. Warner, M. B. Cohen, and B. J. Aronow.** 2002. Novel genes and functional relationships in the adult mouse gastrointestinal tract identified by microarray analysis. Gastroenterology **122:**1467–1482.
5. **Bedard, K., and K. H. Krause.** 2007. The NOX family of ROS-generating NADPH oxidases: physiology and pathophysiology. Physiol. Rev. **87:**245–313.
6. **Bedogni, B., J. A. Warneke, B. J. Nickoloff, A. J. Giaccia, and M. B. Powell.** 2008. Notch1 is an effector of Akt and hypoxia in melanoma development. J. Clin. Invest. **118:**3660–3670.
7. **Block, K., A. Eid, K. K. Griendling, D. Y. Lee, Y. Wittrant, and Y. Gorin.** 2008. Nox4 NAD(P)H oxidase mediates Src-dependent tyrosine phosphorylation of PDK-1 in response to angiotensin II: role in mesangial cell hypertrophy and fibronectin expression. J. Biol. Chem. **283:**24061–24076.
8. **Crosnier, C., D. Stamataki, and J. Lewis.** 2006. Organizing cell renewal in the intestine: stem cells, signals and combinatorial control. Nat. Rev. Genet. **7:**349–359.
9. **de Lau, W., N. Barker, and H. Clevers.** 2007. WNT signaling in the normal intestine and colorectal cancer. Front. Biosci. **12:**471–491.
10. **Espinosa, L., J. Ingles-Esteve, C. Aguilera, and A. Bigas.** 2003. Phosphorylation by glycogen synthase kinase-3 beta down-regulates Notch activity, a link for Notch and Wnt pathways. J. Biol. Chem. **278:**32227–32235.
11. **Fre, S., M. Huyghe, P. Mourikis, S. Robine, D. Louvard, and S. Artavanis-Tsakonas.** 2005. Notch signals control the fate of immature progenitor cells in the intestine. Nature **435:**964–968.
12. **Fukumoto, S., C. M. Hsieh, K. Maemura, M. D. Layne, S. F. Yet, K. H. Lee, T. Matsui, A. Rosenzweig, W. G. Taylor, J. S. Rubin, M. A. Perrella, and M. E. Lee.** 2001. Akt participation in the Wnt signaling pathway through Dishevelled. J. Biol. Chem. **276:**17479–17483.
13. **Fukuyama, M., K. Rokutan, T. Sano, H. Miyake, M. Shimada, and S. Tashiro.** 2005. Overexpression of a novel superoxide-producing enzyme, NADPH oxidase 1, in adenoma and well differentiated adenocarcinoma of the human colon. Cancer Lett. **221:**97–104.
14. **Garg, P., A. Ravi, N. R. Patel, J. Roman, A. T. Gewirtz, D. Merlin, and S. V. Sitaraman.** 2007. Matrix metalloproteinase-9 regulates MUC-2 expression through its effect on goblet cell differentiation. Gastroenterology **132:**1877–1889.
15. **Gavazzi, G., B. Banfi, C. Deffert, L. Fiette, M. Schappi, F. Herrmann, and K. H. Krause.** 2006. Decreased blood pressure in NOX1-deficient mice. FEBS Lett. **580:**497–504.
16. **Geiszt, M., K. Lekstrom, S. Brenner, S. M. Hewitt, R. Dana, H. L. Malech, and T. L. Leto.** 2003. NAD(P)H oxidase 1, a product of differentiated colon epithelial cells, can partially replace glycoprotein 91phox in the regulated production of superoxide by phagocytes. J. Immunol. **171:**299–306.
17. **He, X. C., T. Yin, J. C. Grindley, Q. Tian, T. Sato, W. A. Tao, R. Dirisina, K. S. Porter-Westpfahl, M. Hembree, T. Johnson, L. M. Wiedemann, T. A. Barrett, L. Hood, H. Wu, and L. Li.** 2007. PTEN-deficient intestinal stem cells initiate intestinal polyposis. Nat. Genet. **39:**189–198.
18. **He, X. C., J. Zhang, W. G. Tong, O. Tawfik, J. Ross, D. H. Scoville, Q. Tian, X. Zeng, X. He, L. M. Wiedemann, Y. Mishina, and L. Li.** 2004. BMP signaling inhibits intestinal stem cell self-renewal through suppression of Wnt-beta-catenin signaling. Nat. Genet. **36:**1117–1121.
19. **Jenny, M., C. Uhl, C. Roche, I. Duluc, V. Guillermin, F. Guillemot, J. Jensen, M. Kedinger, and G. Gradwohl.** 2002. Neurogenin3 is differentially required for endocrine cell fate specification in the intestinal and gastric epithelium. EMBO J. **21:**6338–6347.
20. **Jensen, J., E. E. Pedersen, P. Galante, J. Hald, R. S. Heller, M. Ishibashi, R. Kageyama, F. Guillemot, P. Serup, and O. D. Madsen.** 2000. Control of endodermal endocrine development by Hes-1. Nat. Genet. **24:**36–44.
21. **Juhasz, A., Y. Ge, S. Markel, A. Chiu, L. Matsumoto, J. van Balgooy, K. Roy, and J. H. Doroshow.** 2009. Expression of NADPH oxidase homologues and accessory genes in human cancer cell lines, tumours and adjacent normal tissues. Free Radic. Res. **43:**523–532.
22. **Kawahara, T., Y. Kuwano, S. Teshima-Kondo, R. Takeya, H. Sumimoto, K. Kishi, S. Tsunawaki, T. Hirayama, and K. Rokutan.** 2004. Role of nicotinamide adenine dinucleotide phosphate oxidase 1 in oxidative burst response to Toll-like receptor 5 signaling in large intestinal epithelial cells. J. Immunol. **172:**3051–3058.
23. **Kikuchi, H., M. Hikage, H. Miyashita, and M. Fukumoto.** 2000. NADPH oxidase subunit, gp91(phox) homologue, preferentially expressed in human colon epithelial cells. Gene **254:**237–243.
24. **Kim, S., C. Domon-Dell, Q. Wang, D. H. Chung, A. Di Cristofano, P. P. Pandolfi, J. N. Freund, and B. M. Evers.** 2002. PTEN and TNF-alpha regulation of the intestinal-specific Cdx-2 homeobox gene through a PI3K, PKB/Akt, and NF-kappaB-dependent pathway. Gastroenterology **123:**1163–1178.
25. **Korinek, V., N. Barker, P. Moerer, E. van Donselaar, G. Huls, P. J. Peters, and H. Clevers.** 1998. Depletion of epithelial stem-cell compartments in the small intestine of mice lacking Tcf-4. Nat. Genet. **19:**379–383.
26. **Kotelevets, L., J. van Hengel, E. Bruyneel, M. Mareel, F. van Roy, and E. Chastre.** 2005. Implication of the MAGI-1b/PTEN signalosome in stabilization of adherens junctions and suppression of invasiveness. FASEB J. **19:**115–117.
27. **Langlois, M. J., S. A. Roy, B. A. Auclair, C. Jones, F. Boudreau, J. C. Carrier, N. Rivard, and N. Perreault.** 2009. Epithelial phosphatase and tensin homolog regulates intestinal architecture and secretory cell commitment and acts as a modifier gene in neoplasia. FASEB J. **23:**1835–1844.
28. **Laurent, E., J. W. McCoy III, R. A. Macina, W. Liu, G. Cheng, S. Robine, J. Papkoff, and J. D. Lambeth.** 2008. Nox1 is over-expressed in human colon cancers and correlates with activating mutations in K-Ras. Int. J. Cancer **123:**100–107.
29. **Lee, S. R., K. S. Yang, J. Kwon, C. Lee, W. Jeong, and S. G. Rhee.** 2002. Reversible inactivation of the tumor suppressor PTEN by H2O2. J. Biol. Chem. **277:**20336–20342.
30. **Leslie, N. R., D. Bennett, Y. E. Lindsay, H. Stewart, A. Gray, and C. P. Downes.** 2003. Redox regulation of PI 3-kinase signalling via inactivation of PTEN. EMBO J. **22:**5501–5510.
31. **Leteurtre, E., V. Gouyer, K. Rousseau, O. Moreau, A. Barbat, D. Swallow, G. Huet, and T. Lesuffleur.** 2004. Differential mucin expression in colon carcinoma HT-29 clones with variable resistance to 5-fluorouracil and methotrexate. Biol. Cell **96:**145–151.
32. **Leto, T. L., and M. Geiszt.** 2006. Role of Nox family NADPH oxidases in host defense. Antioxid. Redox Signal. **8:**1549–1561.
33. **Liu, C., Y. Li, M. Semenov, C. Han, G. H. Baeg, Y. Tan, Z. Zhang, X. Lin, and X. He.** 2002. Control of beta-catenin phosphorylation/degradation by a dual-kinase mechanism. Cell **108:**837–847.
34. **Lu, Y., and L. M. Wahl.** 2005. Oxidative stress augments the production of matrix metalloproteinase-1, cyclooxygenase-2, and prostaglandin E2 through enhancement of NF-kappa B activity in lipopolysaccharide-activated human primary monocytes. J. Immunol. **175:**5423–5429.
35. **Marsh, V., D. J. Winton, G. T. Williams, N. Dubois, A. Trumpp, O. J. Sansom, and A. R. Clarke.** 2008. Epithelial Pten is dispensable for intestinal homeostasis but suppresses adenoma development and progression after Apc mutation. Nat. Genet. **40:**1436–1444.
36. **McManus, E. J., K. Sakamoto, L. J. Armit, L. Ronaldson, N. Shpiro, R. Marquez, and D. R. Alessi.** 2005. Role that phosphorylation of GSK3 plays in insulin and Wnt signalling defined by knockin analysis. EMBO J. **24:**1571–1583.
37. **Mesquita, P., N. Jonckheere, R. Almeida, M. P. Ducourouble, J. Serpa, E. Silva, P. Pigny, F. S. Silva, C. Reis, D. Silberg, I. Van Seuningen, and L. David.** 2003. Human MUC2 mucin gene is transcriptionally regulated by Cdx homeodomain proteins in gastrointestinal carcinoma cell lines. J. Biol. Chem. **278:**51549–51556.
38. **Milano, J., J. McKay, C. Dagenais, L. Foster-Brown, F. Pognan, R. Gadient, R. T. Jacobs, A. Zacco, B. Greenberg, and P. J. Ciaccio.** 2004. Modulation of notch processing by gamma-secretase inhibitors causes intestinal goblet cell metaplasia and induction of genes known to specify gut secretory lineage differentiation. Toxicol. Sci. **82:**341–358.
39. **Mutoh, H., H. Sakamoto, H. Hayakawa, Y. Arao, K. Satoh, M. Nokubi, and K. Sugano.** 2006. The intestine-specific homeobox gene Cdx2 induces expression of the basic helix-loop-helix transcription factor Math1. Differentiation **74:**313–321.
40. **Nakamura, T., K. Tsuchiya, and M. Watanabe.** 2007. Crosstalk between Wnt and Notch signaling in intestinal epithelial cell fate decision. J. Gastroenterol. **42:**705–710.
41. **Palomero, T., M. L. Sulis, M. Cortina, P. J. Real, K. Barnes, M. Ciofani, E. Caparros, J. Buteau, K. Brown, S. L. Perkins, G. Bhagat, A. M. Agarwal, G. Basso, M. Castillo, S. Nagase, C. Cordon-Cardo, R. Parsons, J. C. Zuniga-Pflucker, M. Dominguez, and A. A. Ferrando.** 2007. Mutational loss of PTEN induces resistance to NOTCH1 inhibition in T-cell leukemia. Nat. Med. **13:**1203–1210.
42. **Persad, S., A. A. Troussard, T. R. McPhee, D. J. Mulholland, and S. Dedhar.** 2001. Tumor suppressor PTEN inhibits nuclear accumulation of beta-catenin and T cell/lymphoid enhancer factor 1-mediated transcriptional activation. J. Cell Biol. **153:**1161–1174.
43. **Pinto, D., A. Gregorieff, H. Begthel, and H. Clevers.** 2003. Canonical Wnt

signals are essential for homeostasis of the intestinal epithelium. Genes Dev. **17:**1709–1713.
44. **Radtke, F., and H. Clevers.** 2005. Self-renewal and cancer of the gut: two sides of a coin. Science **307:**1904–1909.
45. **Rokutan, K., T. Kawahara, Y. Kuwano, K. Tominaga, K. Nishida, and S. Teshima-Kondo.** 2008. Nox enzymes and oxidative stress in the immunopathology of the gastrointestinal tract. Semin. Immunopathol. **30:**315–327.
46. **Rokutan, K., T. Kawahara, Y. Kuwano, K. Tominaga, A. Sekiyama, and S. Teshima-Kondo.** 2006. NADPH oxidases in the gastrointestinal tract: a potential role of Nox1 in innate immune response and carcinogenesis. Antioxid. Redox Signal. **8:**1573–1582.
47. **Ruel, L., M. Bourouis, P. Heitzler, V. Pantesco, and P. Simpson.** 1993. Drosophila shaggy kinase and rat glycogen synthase kinase-3 have conserved activities and act downstream of Notch. Nature **362:**557–560.
48. **Sadok, A., V. Bourgarel-Rey, F. Gattacceca, C. Penel, M. Lehmann, and H. Kovacic.** 2008. Nox1-dependent superoxide production controls colon adenocarcinoma cell migration. Biochim. Biophys. Acta **1783:**23–33.
49. **Sander, G. R., and B. C. Powell.** 2004. Expression of notch receptors and ligands in the adult gut. J. Histochem. Cytochem. **52:**509–516.
50. **Schonhoff, S. E., M. Giel-Moloney, and A. B. Leiter.** 2004. Neurogenin 3-expressing progenitor cells in the gastrointestinal tract differentiate into both endocrine and non-endocrine cell types. Dev. Biol. **270:**443–454.
51. **Scoville, D. H., T. Sato, X. C. He, and L. Li.** 2008. Current view: intestinal stem cells and signaling. Gastroenterology **134:**849–864.
52. **Shao, M. X., and J. A. Nadel.** 2005. Dual oxidase 1-dependent MUC5AC mucin expression in cultured human airway epithelial cells. Proc. Natl. Acad. Sci. U. S. A. **102:**767–772.
53. **Shao, M. X., and J. A. Nadel.** 2005. Neutrophil elastase induces MUC5AC mucin production in human airway epithelial cells via a cascade involving protein kinase C, reactive oxygen species, and TNF-alpha-converting enzyme. J. Immunol. **175:**4009–4016.
54. **Sheth, P., A. Seth, K. J. Atkinson, T. Gheyi, G. Kale, F. Giorgianni, D. M. Desiderio, C. Li, A. Naren, and R. Rao.** 2007. Acetaldehyde dissociates the PTP1B-E-cadherin-beta-catenin complex in Caco-2 cell monolayers by a phosphorylation-dependent mechanism. Biochem. J. **402:**291–300.
55. **Shin, H. M., L. M. Minter, O. H. Cho, S. Gottipati, A. H. Fauq, T. E. Golde, G. E. Sonenshein, and B. A. Osborne.** 2006. Notch1 augments NF-kappaB activity by facilitating its nuclear retention. EMBO J. **25:**129–138.
56. **Suh, Y. A., R. S. Arnold, B. Lassegue, J. Shi, X. Xu, D. Sorescu, A. B. Chung, K. K. Griendling, and J. D. Lambeth.** 1999. Cell transformation by the superoxide-generating oxidase Mox1. Nature **401:**79–82.
57. **Szanto, I., L. Rubbia-Brandt, P. Kiss, K. Steger, B. Banfi, E. Kovari, F. Herrmann, A. Hadengue, and K. H. Krause.** 2005. Expression of NOX1, a superoxide-generating NADPH oxidase, in colon cancer and inflammatory bowel disease. J. Pathol. **207:**164–176.
58. **Torres, J., and R. Pulido.** 2001. The tumor suppressor PTEN is phosphorylated by the protein kinase CK2 at its C terminus. Implications for PTEN stability to proteasome-mediated degradation. J. Biol. Chem. **276:**993–998.
59. **Tsuchiya, K., T. Nakamura, R. Okamoto, T. Kanai, and M. Watanabe.** 2007. Reciprocal targeting of Hath1 and beta-catenin by Wnt glycogen synthase kinase 3beta in human colon cancer. Gastroenterology **132:**208–220.
60. **Valente, A. J., Q. Zhou, Z. Lu, W. He, M. Qiang, W. Ma, G. Li, L. Wang, B. Banfi, K. Steger, K. H. Krause, R. A. Clark, and S. Li.** 2008. Regulation of NOX1 expression by GATA, HNF-1alpha, and Cdx transcription factors. Free Radic. Biol. Med. **44:**430–443.
61. **van Es, J. H., M. E. van Gijn, O. Riccio, M. van den Born, M. Vooijs, H. Begthel, M. Cozijnsen, S. Robine, D. J. Winton, F. Radtke, and H. Clevers.** 2005. Notch/gamma-secretase inhibition turns proliferative cells in intestinal crypts and adenomas into goblet cells. Nature **435:**959–963.
62. **Violette, S., E. Festor, I. Pandrea-Vasile, V. Mitchell, C. Adida, E. Dussaulx, J. M. Lacorte, J. Chambaz, M. Lacasa, and T. Lesuffleur.** 2003. Reg IV, a new member of the regenerating gene family, is overexpressed in colorectal carcinomas. Int. J. Cancer **103:**185–193.
63. **Vogelmann, R., M. D. Nguyen-Tat, K. Giehl, G. Adler, D. Wedlich, and A. Menke.** 2005. TGFbeta-induced downregulation of E-cadherin-based cell-cell adhesion depends on PI3-kinase and PTEN. J. Cell Sci. **118:**4901–4912.
64. **Wu, D., and W. Pan.** 2010. GSK3: a multifaceted kinase in Wnt signaling. Trends Biochem. Sci. **35:**161–168.
65. **Yang, Q., N. A. Bermingham, M. J. Finegold, and H. Y. Zoghbi.** 2001. Requirement of Math1 for secretory cell lineage commitment in the mouse intestine. Science **294:**2155–2158.
66. **Yuan, H., J. Mao, L. Li, and D. Wu.** 1999. Suppression of glycogen synthase kinase activity is not sufficient for leukemia enhancer factor-1 activation. J. Biol. Chem. **274:**30419–30423.